

High Temperature Ceramic Fuel Cell Measurement and Diagnostics for Application to Solid Oxide Fuel Cell Systems

T. M. Koehler
D. B. Jarrell
L. J. Bond

October 2001



Prepared for the U.S. Department of Energy
under Contract DE-AC06-76RL01830

DISCLAIMER

This report was prepared as an account of work sponsored by an agency of the United States Government. Neither the United States Government nor any agency thereof, nor Battelle Memorial Institute, nor any of their employees, makes **any warranty, express or implied, or assumes any legal liability or responsibility for the accuracy, completeness, or usefulness of any information, apparatus, product, or process disclosed, or represents that its use would not infringe privately owned rights.** Reference herein to any specific commercial product, process, or service by trade name, trademark, manufacturer, or otherwise does not necessarily constitute or imply its endorsement, recommendation, or favoring by the United States Government or any agency thereof, or Battelle Memorial Institute. The views and opinions of authors expressed herein do not necessarily state or reflect those of the United States Government or any agency thereof.

PACIFIC NORTHWEST NATIONAL LABORATORY
operated by
BATTELLE
for the
UNITED STATES DEPARTMENT OF ENERGY
under Contract DE-AC06-76RL01830

Printed in the United States of America

Available to DOE and DOE contractors from the
Office of Scientific and Technical Information,
P.O. Box 62, Oak Ridge, TN 37831-0062;
ph: (865) 576-8401
fax: (865) 576-5728
email: reports@adonis.osti.gov

Available to the public from the National Technical Information Service,
U.S. Department of Commerce, 5285 Port Royal Rd., Springfield, VA 22161
ph: (800) 553-6847
fax: (703) 605-6900
email: orders@ntis.fedworld.gov
online ordering: <http://www.ntis.gov/ordering.htm>



This document was printed on recycled paper.

High Temperature Ceramic Fuel Cell Measurement and Diagnostics for Application to Solid Oxide Fuel Cell Systems

T. M. Koehler
D. B. Jarrell
L. J. Bond

October 2001

Prepared for
the U.S. Department of Energy
under Contract DE-AC06-76RL01830

Pacific Northwest National Laboratory
Richland, Washington 99352

Summary

There is a growing need for high efficiency, portable and distributed electric power generation. One family of technologies to meet these needs consists of the various forms of fuel cells. This paper is focused on the assessment of sensors and measurement technologies needed to give improved control, diagnostics and data for prognostics for use with high temperature ceramic fuel cells, and for initial demonstration of solid oxide fuel cells (SOFC). This paper also highlights the many challenges and complexities involved with SOFC technology, such as the lack of continuity between research projects, making it difficult to advance the technology in a cooperative manner. Research programs are noted; particularly those that are starting to provide continuity across the wide variety of research projects underway, such as the International Energy Agency.

This paper is the result of an extensive literature review and technology evaluation, performed to determine the status of sensors and measurement technologies. It became apparent that many researchers are trying to overcome the same fuel cell design challenges. All researchers have found it difficult to obtain sound data from measurements inside inaccessible designs and heavily insulated enclosures operating at high temperatures. Although some advancement has been made in materials, systems modeling, and innovative manufacturing techniques, few answers have been found in the measurement and diagnostics field.

Understandably, most approaches to measurements and diagnostics in fuel cells have been to extend an existing practice to solid oxide fuel cells, such as adapting established aqueous electrochemistry techniques (i.e., impedance spectroscopy). Although this technique has manifested some key characteristics of the SOFC, and is arguably one of the most advanced techniques in this field, work is still needed to resolve disagreements on the application and interpretation methods.

Realizing the many constraints involved in SOFC testing and resolved to the fact that simple approaches may not be the complete answer, several innovative techniques and geometries have been tried and included in this report. Many researchers are using a combination of in-situ and ex-situ tests, involving a variety of disciplines and multiple steps to compile a range of diagnostic tools, as well as data acquisition and analysis equipment, which can be adopted to the SOFC technology. This has merit, but requires extensive cooperation between all involved throughout all the stages of the product development. These measurement tools will enable analysis of degradation mechanics leading to development of prognostic tools that can be used to analyze fuel cells and balance of plant (BOP) systems during research and development, subsequently minimizing operating costs and enhancing overall system efficiency.

Acronyms and Abbreviations

ac	Alternating current
AE	Acoustic emission
AlN	Aluminum nitride
AMPS	Affordable Manufacturer of Power Systems
ANL	Argonne National Laboratory
ART	Advanced Refractory Technologies, Inc.
ASR	Area specific resistance
BOP	Balance of plant
C	Celsius
CARS	Coherent Anti-Stokes Raman Spectroscopy
CEPCO	Chubu Electric Power Company, Inc.
CFCL	Ceramic fuel cells
dc	Direct current
DIGIMAPS	Digital Ordnance Survey Maps
DIN	Departmental Identification Number
dp	Differential pressure
E	Ideal equilibrium potential
E°	Ideal standard potential
EC	European Commission
EDAX	Energy dispersive analysis of X-rays
EMF	Electromotive force
EQP	Equipotential
ESPI	Electronic Speckle Pattern Interferometry
EU	European Union
FTIR	Fourier Transform Infrared Spectroscopy
GC	Gas chromatography
GT	Gas turbine
hf	High frequency
IEA	International Energy Agency
IP-SOFC	Integrated Planar-SOFC
IRS	Interscience radial flow
IS	Impedance Spectroscopy
i_{sc}	Short circuit current
ISO	International Standards Organization
kW	Kilowatt
kJ	Kilojoule
LDA	Laser Doppler Anemometry
lf	Low frequency
LHV	Lower heating value
LOCO-SOFC	Low Cost Fabrication-SOFC

LSC	Lanthanum strontium cobaltite
LSCF	Lanthanum strontium cobalt iron
LSM	Lanthanum strontium magnesium oxide
LVDT	Linear variable displacement transformer
MCFC	Molten carbonate fuel cell
MEA	Membrane electrode assemblies
MF	Multifunctional
MHI	Mitsubishi Heavy Industries
MOLB	Mono Block Layer Built design
MPa	Megapascal
MTI	McDermott Technology, Inc.
mV	Millivolts
MW	Megawatt
NETL	National Energy Technology Laboratory
OCV	Open circuit voltage
PEFC	Polymer electrolyte fuel cell
PEM	Proton exchange membrane
PEN	Positive electrolyte negative
PIV	Particle Image Velocimetry
PNNL	Pacific Northwest National Laboratory
pSOFC	Planar SOFC
Pt	Platinum
R&D	Research and development
R_p	Electrode polarization resistance
RE	Reference electrode
Rh	Rhodium
RR	Rolls Royce
R_s	Ohmic resistance
RT	Room temperature
sccg	Sub-critical crack growth
SECA	Solid State Energy Conversion Alliance
SEM	Scanning electron microscope
SOFC	Solid oxide fuel cells
T	Temperature
TMI	Technology Management Inc.
UMR	University of Missouri (Rolla)
XRD	X-ray diffraction
YSZ	Yttria stabilized zirconia

Acknowledgement

The author would like to acknowledge the invaluable assistance of the Don Jarrell, and Leonard Bond, Pacific Northwest National Laboratory, who contributed time, expertise and ideas toward the successful completion of this report. A special thanks to Subhash Singhal, Pacific Northwest National Laboratory, for providing support and sharing his network of contacts.

Contents

Summary	iii
Acronyms and Abbreviations.....	v
Acknowledgement.....	vii
1.0 Summary of Observations.....	1.1
2.0 PNNL Approach to Diagnostics and Prognostics Efforts	2.1
2.1 Introduction.....	2.1
2.2 Task Specific Approach.....	2.1
2.3 Ideal Efficiency	2.2
2.4 Voltage Efficiency	2.6
2.4.1 Activation Polarization (η_{act}).....	2.7
2.4.2 Ohmic Polarization	2.8
2.4.3 Concentration Polarization.....	2.9
2.5 Current Efficiency.....	2.10
2.6 Fuel Efficiency.....	2.10
3.0 Degradation Mechanisms in Planar Designs.....	3.1
3.1 Electrolyte.....	3.1
3.2 Cathode	3.2
3.3 Anode.....	3.2
3.4 Interconnect/Bipolar Plate.....	3.3
3.5 Stressor-degradation Failure	3.3
4.0 Review of SOFC Programs.....	4.1
4.1 Objectives	4.1
4.2 Tubular Versus Planar Designs.....	4.2
4.3 Combination Design Approach.....	4.2
4.4 Planar Design	4.3
5.0 International Energy Agency Collaboration Efforts	5.1
5.1 Introduction.....	5.1
5.2 Thermomechanical Evaluation (Task B2)	5.1
5.3 Instrumentation and Diagnostics (Task B5).....	5.2
6.0 Research Listed by Key Parameters of SOFT Efficiency	6.1
6.1 Evaluation and Testing of Voltage Losses.....	6.1
6.2 Evaluation and Testing of Reactant Utilization	6.7
6.3 Evaluation of Temperature.....	6.11
6.4 Evaluation of Material Testing and Advanced Techniques	6.14
7.0 References.....	7.1

Figures

1. Typical Fuel Cell Balance.....	2.2
2. Fuel Cell Losses.....	2.7
3. Typical Electrochemical Reactions of a SOFC Using Hydrogen and Oxygen.....	3.1
4. Current Interrupt Method Applied to a Fuel Cell.....	6.2
5. Typical Reference Electrode Test Set-Up.....	6.3
6. Sketch of Procedure for Deriving Overpotential Curves.....	6.4
7. General Layout of the Experiment.....	6.20

Tables

1. Mode-Mechanism-Stressor Relationships.....	3.4
---	-----

1.0 Summary of Observations

The objective of this research was to review the status of high temperature ceramic fuel cell technology. Specifically, the focus was on the analytical approaches to planar solid oxide fuel cell (pSOFC) measurement techniques and diagnostics. Many challenges are present in solid oxide fuel cell (SOFC) technology, including those hindering testing such as the high operating temperature and the inaccessibility of the stack and components (without obstruction) of the SOFC process.

These are not only testing challenges, but also design challenges. Combined, they have impeded progress in this technology. Many organizations that have a planar SOFC design are still experimenting to improve material properties, reduce costs, and minimize degradation issues. Other groups chose a different design (that is, tubular) that enabled them to move faster to commercialization; however, as expected, these designs are more difficult to manufacture. Thus, these groups are working to refine their design to facilitate manufacturing and to curtail costs.

As a result of these challenges, tests that can be done on cell components or single cells at room temperature are predominant. Although these tests are necessary to baseline designs when applied to a stack, the failure mechanism often changes. As one researcher pointed out after extensive stress analysis, it is possible that some of the stressors seen in single cells will mitigate others in a stack (Adamson and Travis 1997). In addition, the heat generated in a stack versus a single stack can significantly alter which component degraded and how fast it occurred.

Lack of detailed information and a lack of continuity in the information provided were difficulties encountered during this research and may be responsible for the slow research progress, especially in measurement and diagnostics of SOFC. The missing details of test set-ups resulting in decisive conclusions tend to make the experiments speculative and difficult to compare to other sources. The lack of continuity may be because many of the attempts at fuel cell testing have been new and innovative (beyond accepted standard practices) and as such are difficult to explain and verify. Moreover, many of the tests are accomplished with unique equipment, and, as a result, cannot be commonly practiced without an investment, often a major capital expense. Unfortunately, when a test fails, the reason is not always given (perhaps because it is unknown) and not enough information is provided to resolve the ambiguity.

Another reason for the lack of continuity may be the wide variety of terminology. This variety of terms may be attributed to the many disciplines involved in fuel cell research including, chemists, engineers, electrochemists, and physicists. Each discipline has its own jargon, and uses it to describe, in many cases, the same phenomenon, which can be misleading or confusing. For example, polarization losses are also referred to as the *overpotential* or the *overvoltage*.¹

¹ Overvoltage or overpotential is a term that describes a voltage superimposed over the reversible or ideal voltage. Strictly, this term only applies to differences generated at an electrode interface. A disadvantage of the term is that it implies making voltage larger, whereas in fuel cells, the overvoltage opposes and reduces the reversible ideal voltage (Larminie and Dicks 2000).

The fuel cells are as varied as the research groups. The applications of fuel cells, thus the functionality, can be very different. Subsequently, the fuel cell characteristics are unique with diverse microstructures, electronic behavior, and physical features. This diversity means care must be taken when trying to apply or compare a test procedure or methodology to a different fuel cell. In addition, many organizations have people working on the analogous aspects of fuel cell research from balance of plant systems to material microstructure. The parallel and dynamic micro-to-macro tactics make a literature search that is attempting to ascertain the status of the technology more difficult.

The International Energy Agency (IEA) is one organization that is trying to advance the understanding, development and acceptance of this technology. The program has developed reports that support research efforts. For example, a report called the *Instrumentation and In-Situ Diagnostics: Final Report of Activity B¹* provides information regarding a range of diagnostic approaches that can be used by a variety of researchers in SOFC technology. Programs such as the IEA's provide a method for researchers to enhance their understanding and, in turn, advance the technology.

Accordingly, Pacific Northwest National Laboratory (PNNL) has developed an approach that may fulfill a need noticed by the IEA to develop a systematic procedure for characterization of degradation properties. In this report, PNNL offers a *stressor-degradation-failure approach* and exhibits how this approach can be applied to SOFC technology. Table 1 (in Section 3) displays potential failure modes of SOFC components degradation mechanisms and their corresponding stressors, as well as possible methods to detect them.

¹ IEA publication (not publicly available). A.J. McEvoy. 1996. *Instrumentation and In-Situ Diagnostics: Final Report of Activity B5*. (KFA-IEA) Research Centre Julich-International Energy Agency, Julich, Germany.

2.0 PNNL Approach to Diagnostics and Prognostics Efforts

2.1 Introduction

An aggressive approach to diagnostics is important even in the very early stages of project development. Such an approach provides an integrating framework for the investigation and points the research in a direction that has a higher probability for successful implementation. A systems approach to diagnostic analysis helps to maintain a more pragmatic and balanced perspective. This, in turn, helps to identify and resolve shortcomings in the overall research structure.

Initially, sufficient information was collected to allow an appraisal of what has worked, and not worked, in the world of solid oxide fuel cell measurement and diagnostics. From this task, it became apparent that many researchers are trying to overcome fuel cell design challenges and also the complexity associated with improving the performance of these designs. Moreover, various approaches have been taken to advance SOFC technology including material enhancements, systems modeling, and innovative manufacturing techniques.

As these researchers discovered, many factors affect fuel cell performance, including temperature, pressure, material degradation, and gas composition. Modifications of these factors may improve or reduce the performance of the fuel cell, and changing one factor may inadvertently affect another. For instance, raising fuel cell operating temperature increases performance by increasing the reaction rate and often reduces ohmic resistance of the electrolyte. However, the higher temperatures cause degradation and material problems that may offset these advantages.

In general, to achieve an appropriate fuel cell design for a given application, a tradeoff between operating factors and manufacturing issues may be necessary. For example, high current density design will result in a fuel cell that is compact and typically lower in capital cost. However, inferior system efficiency will result because of a lower cell voltage. This type of compromise may be valid for a mobile application.

2.2 Task Specific Approach

The general approach to diagnostics is founded in the methods of root cause analysis and stressor-degradation correlation. This methodology seeks to derive a quantitative damage rate correlation for known or hypothesized system stressors (refer to the stressor-degradation-failure discussion in Section 3).

The diagnostics approach was to concentrate on the elements of mass and energy balances for a planar SOFC design to identify the critical parameters for measurement. In addition, it would identify the key parameters that detrimentally affect the efficiency of a SOFC. Subsequently, a determination was made to observe which parameters can be directly or indirectly measured in a half-cell and/or stack of cells and which must be derived through analytical relationships.

For example, a mass balance would entail measuring the reactants and products of a system, such as depicted in the following equation: $2\text{H}_2 + \text{O}_2 \rightarrow 2\text{H}_2\text{O}$, for a SOFC operating on hydrogen fuel. The hydrogen (H), oxygen (O) and water (H_2O) can be measured directly via the tubing entering and leaving the fuel cell system. However, the amount of fuel or oxygen that leaks out of the fuel cell system will not be detected by these direct measurements and will have to be determined by another method.

As Figure 1 depicts, the SOFC cell reaction involves fuel and oxygen as inputs with electricity, water, and heat as outputs. As stated previously, these terms can be measured directly or determined from other parameters, such as the voltage and current of the total fuel cell stack, which (as primary indicators of cell performance) are always measured directly. When the current and voltage are known, the power can be determined, based on the equation:

$$\text{Power, } P = V * I * n_s$$

where n_s = number of cells in a stack.

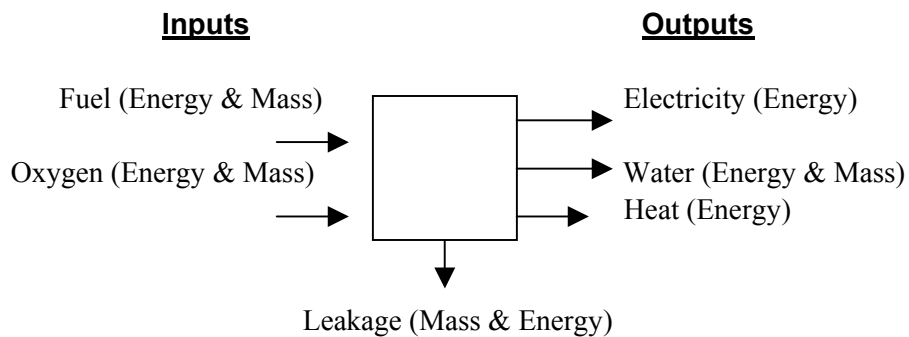


Figure 1. Typical Fuel Cell Balance

As stated, to completely analyze a fuel cell system, a mass and energy balance, as well as efficiency characteristics must be reviewed. The efficiency of the fuel cell gives insight to how the key elements of the fuel cell behave as a unit.

2.3 Ideal Efficiency

The overall electrical conversion efficiency of a fuel cell system is defined as the outgoing electrical power divided by the chemical energy going into the fuel cell. To explain how the ideal efficiency is derived, an example of a hydrogen-supplied fuel cell is used. For a hydrogen fuel cell, the overall fuel cell equation is:



The product is one mole of water (H₂O) and the reactants are one mole of hydrogen (H₂) and a half mole of oxygen (O).

Thus, another equation describing the energy released for this reaction in terms of Gibbs free energy of formation (in molar form, \hat{g}) can be written as

$$\Delta \hat{g}_f = (\hat{g}_f)_{\text{H}_2\text{O}} - (\hat{g}_f)_{\text{H}_2} - \frac{1}{2} (\hat{g}_f)_{\text{O}_2}$$

If this reaction were reversible or ideal (that is, no losses in the fuel cell), all the Gibbs free energy released could be converted into electrical energy. In practice, the reaction is not adiabatic (because heat is released) and this is typically denoted as a negative sign before the Gibbs free energy symbol.

The electrical energy that would be created in this ideal reaction could be calculated in the following manner:

- For every one molecule of hydrogen and water, two electrons transport around the external circuit, creating a charge

$$[2N_a * \text{charge per electron}] = 2 * (N_a * e) = 2 (F) \text{ \{Coulombs\}}$$

where $N_a = \text{Avogadro's \#}^1$
 $e = \text{charge on one electron}^2$
 $F = \text{Faraday constant}^3$

- If $V_{oc} = \text{voltage}$, then electrical work done = (charge) * voltage = $-(2F) * V_{oc}$ \{Joules\}.
- An ideal reaction with no losses means that the electrical work done equals $\Delta \hat{g}_f = -(2F) * V_{oc}$
- Changing the equation around in terms of voltage results in $E = V_{oc} = -\Delta \hat{g}_f / 2F$. This equation describes the electrometric force (EMF, denoted as E) or reversible open circuit voltage (OCV) of a hydrogen fuel cell.
- A general form of the equation for any fuel cell is developed by changing the number “2” in the denominator to a variable z, yielding

$$E = -\Delta \hat{g}_f / zF$$

where z = is the number of electrons transferred for each molecule of fuel (Larminie and Dicks 2000) and the negative sign indicates the reaction releases energy.

¹ Avogadro's number states that 1 mole of any perfect gas contains the same number of molecules: 6.022×10^{23} molecules/gmole, or 2.73×10^{26} molecules/pmole.

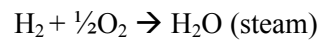
² Charge on one electron = -1.602×10^{19} Coulombs.

³ Faraday's constant = 9.648×10^4 Coulombs/gmole.

However, as mentioned previously, the reaction is not without losses. In addition, Gibbs free energy of formation is not constant, but varies with temperature, reactant pressure, and concentration. The understanding and optimizing of these parameters is critical to the efficiency of the fuel cell.

The Nernst¹ equation is key to understanding the fuel cell. It gives EMF or the reversible open circuit voltage in terms of product and/or reactant activity. Moreover, the Nernst equation provides a relationship between the ideal standard² potential³ (E^0) for the cell reaction and the ideal equilibrium potential (E) at other temperatures and partial pressures of reactants and products. Consequently, given the ideal potential at standard conditions, the ideal voltage can be determined at other temperatures and pressures. For instance, the ideal standard potential (E^0) of a hydrogen fueled cell with a liquid water product is 1.23 volts and the ideal potential (E) for a SOFC operating on hydrogen at 1100°C is 0.91 volts (Hirschenhofer et al. 1998).

Again citing a hydrogen supplied fuel cell with an overall fuel cell equation of



This equation can be written as⁴

$$\Delta g_f = -\Delta g_f^0 - RT * \ln [a_{\text{H}_2} * a_{\text{O}_2}^{1/2} / a_{\text{H}_2\text{O}}]$$

where a = activities of the reactants and products and Δg_f^0 is the change in molar Gibbs free energy of formation at standard pressure. Using the ideal gas laws (assuming steam acts like an ideal gas),

$$a_{\text{H}_2} = P_{\text{H}_2} / P^0, \quad a_{\text{O}_2} = P_{\text{O}_2} / P^0 \quad \text{and} \quad a_{\text{H}_2\text{O}} = P_{\text{H}_2\text{O}} / P^0$$

and substituting into the equation ($E = -\Delta g_f / 2F$, given P^0 = standard pressure or 1 bar) yields:

$$E = E^0 + RT/2F * \ln [P_{\text{H}_2} * P_{\text{O}_2}^{1/2} / P_{\text{H}_2\text{O}}]$$

where all pressures are given in bar and P = gas partial pressure. This equation is a form of the Nernst equation that relates fuel cell voltage to products and reactants, while providing a basis for quantitative analysis of the fuel cell.

¹ The Nernst equation, developed by German chemist Walther Nernst, is a mathematical statement of the electrochemical potential of a system.

² Standard conditions are 1 atmosphere and 25°C (77°F).

³ The standard Nernst potential is the ideal cell voltage at standard conditions without any cell losses and as such, can be considered the open circuit voltage.

⁴ Thermodynamic arguments given as a reference in Larminie and Dicks (2000) as 'Balmer R. (1990) *Thermodynamics*, West'.

Another relationship that describes fuel cell performance is the efficiency in terms of combustion. The maximum efficiency (often called the thermodynamic efficiency) of a fuel cell includes the combustion term, enthalpy of formation¹ and is given by the following equation:

$$\Delta \hat{g}_f / \Delta \hat{h}_f * 100 \text{ percent, where } \Delta \hat{h}_f = \text{enthalpy of formation}$$

For example, in the hydrogen fuel cell reaction, at 25°C (liquid product), $\Delta \hat{h}_f = 285.84$ kJ/mole, and $\Delta \hat{g}_f = 237.2$ kJ/mole with a maximum efficiency of 83 percent (Larminie and Dicks 2000).

Thus, the thermal efficiency of this fuel cell, in terms of actual voltage, can be written as

$$\eta = \text{Useful power}/(\Delta G/0.83) = \{(V_{\text{actual}} * \text{Current}) / (\text{Volts}_{\text{ideal}}/\text{Current}/0.83)\} = (0.83 * (V_{\text{actual}}/V_{\text{ideal}}))$$

Further, as stated earlier, the ideal voltage of a hydrogen fueled cell is 1.23 volts; therefore, the thermal efficiency of a cell operating at a voltage V_{cell} is given by (Hirschenhofer et al. 1998)

$$\eta = (0.83 * V_{\text{actual}}) / V_{\text{ideal}} = (0.83 * V_{\text{actual}} / 1.23) = 0.675 * V_{\text{cell}}$$

The derivation and understanding of these relationships provide the basis for fuel cell evaluation.

To evaluate the efficiency of a fuel cell system, it is dissected into various terms. The overall electrical conversion efficiency (η_E) of a fuel cell system can be shown by the following equation:

$$\eta_E = \eta_{\text{ideal}} * \eta_v * \eta_i * \eta_u * \eta_s * \eta_{fp} * \epsilon_{fp}$$

where η_{ideal} = ideal or reversible efficiency, η_v = voltage efficiency, η_i = current efficiency, η_u = fuel efficiency, η_s = system efficiency, η_{fp} = fuel heating value efficiency, and ϵ_{fp} = mass flow rate efficiency (Ellis 2000).

The last three terms; system efficiency (η_s), fuel heating value efficiency (η_{fp}), and mass flow rate efficiency, (ϵ_{fp}) include losses considered in the balance of the plant. The system efficiency refers to the fact that some of the electricity generated may be used within the fuel cell system and may not contribute to the total system electrical output. The last two terms relate to losses of the fuel processor itself. Because this research focused on the testing and losses associated with only the fuel cell, the losses associated with these last three terms are not discussed further.

¹ Enthalpy of formation is the energy released or absorbed by an element or compound taking part in a reaction. It depends on the phase of the compound, and is assigned a value of zero for elements in free states. It can be calculated by summing enthalpies of reactants over all products (Lindeburg 1990).

2.4 Voltage Efficiency

The voltage efficiency (η_v) is defined as the net voltage (voltage decreased from its equilibrium potential as a result of irreversible losses) divided by the maximum voltage. The voltage losses are attributed to polarization losses that primarily originate from three sources: concentration, activation, and ohmic polarizations. Thus, the net cell voltage is the open circuit voltage, minus the various polarization losses, and can be written as:

$$V_{\text{cell}} = V_{\text{open}} - V_{\text{act}} - V_{\text{ohm}} - V_{\text{conc}}$$

The following equations are used to describe the polarizations (voltage losses):

$$\eta = \eta_{\text{act}} + \eta_{\text{ohm}} + \eta_{\text{conc}}$$

The activation polarization equation¹ is:

$$\eta_{\text{act}} = RT/nF\alpha * \ln(i/i_o)$$

where α = electron transfer coefficient², F = Faraday's constant, n = electrons involved in the transfer, R = gas constant, T = temperature, i_o = exchange current density³ and i = current density.

The ohmic polarization equation is:

$$\eta_{\text{ohm}} = ir$$

where i = current density and r = area specific resistance (ASR).

The concentration polarization equation is:

$$\eta_{\text{conc}} = RT/nF * (1 - i/i_L)$$

where F = Faraday's constant, n = electrons involved in the reaction, R = gas constant, T = temperature, i = current density and i_L = limiting current.

The equation for all losses combined would be:

$$V_{\text{cell}} = E - \{RT/nF\alpha * \ln(i/i_o)\} - ir - \{RT/nF * (1 - i/i_L)\}$$

¹ The activation polarization equation is also called the Tafel equation and is only valid when $i > i_o$ (Larminie and Dicks 2000).

² Electron transfer coefficient is also called the "charge transfer coefficient" and is the proportion of electrical energy applied that is harnessed in changing the rate of an electrochemical reaction. The value of the electron transfer coefficient depends on the material the electrode and the reaction involved. (Larminie and Dicks 2000).

³ The exchange current density is the current density caused by the continual flow of electrons to and from the electrolyte in a given fuel cell. It indicates the amount of "activity" at the surface of the electrodes (Larminie and Dicks 2000).

2.4.1 Activation Polarization

As seen in Figure 2, the activation polarization (η_{act}) is nonlinear and dominant at low current density. The activation polarization is related to a physical or electrical barrier at the surface (interfaces) of the electrodes. The term is used to indicate the activation energy needed to overcome the resistance of the slowest step in the reaction. At the anode and the cathode, reactants diffuse to reaction sites, where the reduction and oxidation take place. At these sites, the activation potential (voltage difference) must be overcome before the reaction can proceed. It is also referred to as a voltage drop because a portion of the voltage generated is lost in driving the chemical reaction. This type of loss is expected to be the largest of

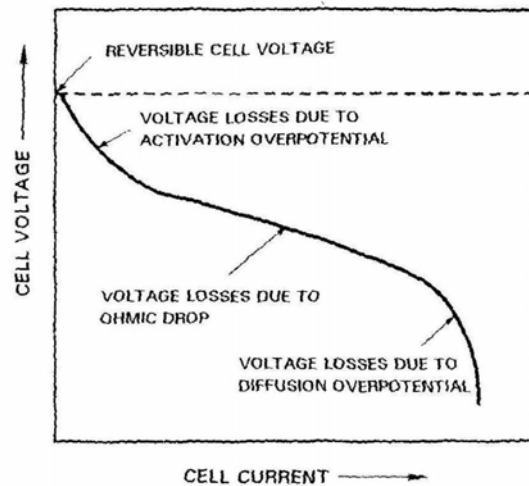


Figure 2. Fuel Cell Losses

the three polarizations in low and medium temperature fuel cells and is usually caused by the cathode. Catalysts are often used to overcome the activation potential and allow the reaction to proceed. At higher temperatures (considered to be $>800^{\circ}\text{C}$) in fuel cells, the activation potential is lower and generally does not need a catalyst. If a cell is using a fuel other than hydrogen, both electrodes are likely to exhibit significant activation polarization losses.

The charge double layer is a layer of charge caused by the attraction of ions and electrons, on or near an electrode-electrolyte interface (Larminie and Dicks 2000). This layer is a store of energy that behaves like a capacitor, that is, if the current changes, the charge and corresponding voltage needs time to dissipate or increase, accordingly. This is often considered one explanation for the occurrence of the activation polarization.

The activation polarization (η_{act}) equation is also known as the Tafel equation. It was experimentally proven by Tafel that in most electrochemical reactions, a plot of overvoltage against the log of current density results in a straight-line relationship. The $(RT/nF\alpha)$ term is a constant that is higher for an electrochemical reaction that is slow, and i_0 (the current density at which the voltage moves from zero) is higher, if the reaction is fast. The current density (i_0) that is also called the exchange current density (Larminie and Dicks 2000), can be described as the flow of electrons from and to the electrolyte. It is critical for this current density to be as high as possible because it is easier to keep a process going and just switch directions than to start a flow moving from scratch. The exchange current density is the parameter in the activation polarization equation that exhibits the most variation (Larminie and Dicks 2000).

Many methods are known and under investigation that can reduce activation polarization, such as raising cell temperature, doping the electrode with effective catalysts, increasing the surface area of the electrode by making it rougher, increasing reactant concentration (using pure O_2 instead of air, in an attempt to force reactants to occupy catalyst sites more effectively), and by increasing the pressure. The method of increasing pressure is presumed to work by increasing catalyst site occupancy, which increases the open circuit voltage (Larminie and Dicks 2000).

2.4.2 Ohmic Polarization

Unlike the activation and concentration polarization, the ohmic polarization (η_{ohm}) is a linear function of the cell current and, as depicted in Figure 2, increases over the entire range of current.

The ohmic polarization refers to the voltage drop caused by the resistance, which is fairly constant in a given cell, to the flow of electrons and ions through the cell. Typically, the ohmic polarization is caused by the electrolyte, the cell interconnectors or bipolar plates. In the equation ($V_{ohm} = i * r$), the current is often expressed as current density (amps per area, such as mA/cm^2) to be consistent with the other equations. Therefore, the resistance in the equation is a resistance per 1 cm^2 (with typical units of $k\text{-ohm/cm}^2$), denoted as a small r , and called area specific resistance (ASR).

The ohmic polarization is especially important in SOFC. Some of the methods used to reduce this resistance include:

- choose electrodes with high conductivity
- choose appropriate bipolar plate/interconnect materials that are low in ohmic resistance and that complement the other cell component materials
- make the electrolyte thin, but structurally stable, with the ability to prevent shorting from one electrode to the other.

2.4.3 Concentration Polarization

The concentration polarization (η_{conc}) shown in Figure 2, dominates at high current density. It is related to diffusion (a chemical barrier/ion depletion) and is often referred to as a mass transport loss because the reduction of concentration is the result of a failure to transport sufficient reactant to the electrode surface. As current density increases, the required flow rate of reactants to sustain the reaction also increases. Eventually, the rate of transport through the cell cannot keep up with the rate at which the reactants are consumed. The concentration of reactants at the reaction sites begins to drop and, thus, voltage drops.

At the cathode, as oxygen is being used (typically from an air supply), a reduction in the concentration of oxygen in the region of the electrode occurs. This change in concentration causes a drop in the partial pressure of the oxygen; how extreme the drop depends on the current being taken from the fuel cell. Other dependencies are the physical characteristics of the fuel cell, such as how well the air supply circulates to replenish the oxygen. Similarly, at the anode as hydrogen is used and current is generated, a drop in gas pressure occurs. As with the cathode, the rate of this drop will depend on the characteristics of the fuel cell, such as the gas supply system. The supply system will consist of channels the gas will flow through and this flow will result in a pressure drop as a result of channel fluid resistance.

The equation for concentration losses can be studied by considering the case at the cathode, where the change in pressure caused by the use of the fuel gas caused a drop in voltage. The equation would be:

$$\eta_{\text{conc}} = RT/nF * \ln(P_2/P_1)$$

This equation can be transformed into another useful relationship by considering the case when the current density of the fuel cell will be constrained by how fast the fuel can be supplied to electrode. If i_L is the limiting current density that corresponds to this maximum rate of fuel usage and P_1 is the pressure when the current density is zero, and assuming that the pressure will fall linearly down to zero at the current density i , then pressure P_2 , at any current density i , would be $P_2 = P_1(1-i/i_L)$ (Larminie and Dicks 2000). By substitution into the equation above, the result is the Nernst equation given earlier (in section 2.4)

$$\Delta V = - RT/nF * \ln((1-i/i_L))$$

This equation displays voltage change caused by mass transport losses, (with a negative sign added to indicate a voltage drop). This equation gives a good formula for the mass transport voltage drop for the entire cell since at either of the electrodes the current density (i) can reach the limiting current density (i_L) causing the entire cell voltage to drop to zero. One caveat to this last statement is that for it to be true, the actual value of the term denoted as “ RT/nF ” (which will vary with different fuel cell reactants) must be larger than the theoretical value.

The important factor to remember about these polarizations is that they do not act independently of each other. A change in partial pressure that affects the concentration polarization will also affect the activation polarization.

2.5 Current Efficiency

The current efficiency (η_i) can be defined by the following equation (Ellis 2000)

$$\eta_i = I_{\text{cell}} / n N * F$$

where I_{cell} = actual cell current, divided by the terms in the denominator that represent the ideal cell current. The denominator terms are, n = electrons involved in the reaction, F = Faraday's constant, and N = molar rate of reaction of the fuel (mol/sec).

The current efficiency can be stated as the percent of current passing through an electrolytic cell (or electrode) that accomplishes the desired chemical reaction, compared to the ideal case. For example, in the hydrogen fuel cell, ideally every hydrogen (H_2) molecule would react to produce two electrons that would contribute to the current flow. The inefficiencies arise from reactions other than the intended one taking place at the electrodes, or the side reactions consuming the current. Some hydrogen for instance, may go through the electrolyte and not react at all, or the hydrogen does react but the produced current is driven through the electrolyte and never contributes to the current flow.

2.6 Fuel Efficiency

Fuel efficiency (η_u) is defined by the following equation:

$$\eta_u = N / N_a$$

where N = molar rate of reaction of the fuel removed from the anode stream as a result of a chemical reaction (mol/sec) and N_a = molar rate of reaction of the fuel supply into the anode (mol/sec) (Ellis 2000).

The fuel utilization losses occur because some of the fuel may react electrochemically, but not generate power as a result of taking another pathway out of the cell (such as in leakage), thus not be measured at the exit of the anode stream.

3.0 Degradation Mechanisms in Planar Designs

3.1 Electrolyte

As shown in Figure 3, the basic SOFC involves two major flow paths; an internal path of negatively charged oxygen ions that flow through the electrolyte and an external path of electrons that generate electricity. The electrolyte must be stable in the reducing and the oxidizing environments; it must also allow the oxygen ions to flow from the air electrode (cathode) to the fuel electrode (anode), where the ions can react with the fuel. The electrolyte material should be free of porosity so gases cannot permeate across it, be uniformly thin to reduce ohmic losses, and have high ion conductivity with a transference number for oxygen ions close to unity (one) and a transference number for electrons close to zero.

Most researchers use yttria (yttrium oxide, Y_2O_3) stabilized zirconia (zirconium oxide, ZrO_2) as the electrolyte as a result of its stability over the oxygen partial pressures and oxygen transference number of one¹.

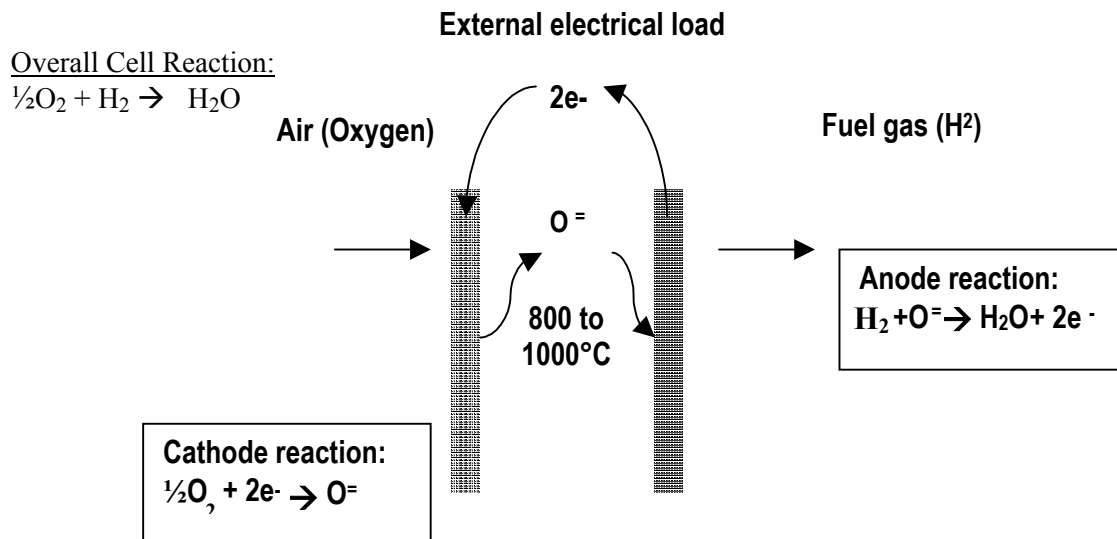


Figure 3. Typical Electrochemical Reactions of a SOFC Using Hydrogen and Oxygen

¹ Transference Number: The transference number of an ion is the fraction of the total current that is carried by that ion during electrolysis. Different ions carry different fractions of the current because different ions move at different speeds under the same potential gradient.

The thickness of the electrolyte is dependent on whether the design is electrolyte supported or electrode supported. Typically, in an electrolyte-supported cell, the thickness of the electrolyte is in the 50- to 150- μm range, yielding a high ohmic resistance, and making the design suitable for approximately 1000°C operation. In an electrode-supported cell, the electrolyte can be thinner, in the range of 5 to 20 μm and more suitable for lower temperature operation (Singhal 2001).

3.2 Cathode

The cathode functions on the oxygen (usually supplied by air) side of the fuel cell in an oxidizing environment. In other words, oxygen as a gas is reduced to oxygen ions by transferring electrons. Because this electron transfer takes place on the surface of the electrode, the surface area is a very important parameter of the design. In fact, the rate at which this transfer occurs is designated in the units of current per area.

The desired material characteristics include high electronic conductivity, thermal expansion compatibility, and adequate porosity to provide a sufficient electrode-electrolyte interfacial region for electrochemical reaction. In addition, the cathode material must provide a good interface without forming troublesome reactions with other materials.

Many materials are being considered as cathode material, such as LSM ($\text{La}_{0.9}\text{Sr}_{0.1}\text{MnO}_3$). Unfortunately, testing has uncovered a variety of these deleterious reactions, such as manganese (Mn) diffusing with the zirconia and forming an electronic shorting throughout the electrolyte or the cathode material reacting with the zirconia electrolyte to form a compound ($\text{La}_2\text{Zr}_2\text{O}_7$) that is electrically insulating (Khandkar, Elangovan, and Hartvigsen 1996). To overcome these problems, extensive research has gone into the preparation of the materials, especially the sintering process. Some researchers have even included an interlayer (that acts like a buffer) during fabrication to inhibit these types of reactions between the electrolyte and the cathode.

3.3 Anode

The anode material must be stable in reducing atmospheres and electronic conduction. In addition, the porosity of the anode must allow the transport of the fuel to the electrolyte/fuel electrode interface where fuel oxidation takes place, and must allow the products of the oxidation to move away from the interface region. As previously mentioned, this transfer takes place at the surface of the anode, thus area is a critical design parameter. The porosity of the electrodes, in effect, increases the surface area by providing more potential reactant sites.

The atmosphere is reducing, thus metals are often used, such as nickel in Ni-ZrO₂. In this combination, the nickel component is catalytic to hydrogen oxidation and hydrocarbon fuel reforming; the zirconia keeps the nickel from coarsening at the high operating temperatures that could detrimentally reduce the porosity of the anode. In addition, nickel has a larger thermal expansion coefficient than yttria stabilized zirconia (YSZ); thus the zirconia keeps down the bulk thermal expansion of the total anode. It

is also thought the zirconia may provide an extension of the three-phase boundary for the electrochemical reaction (Khandkar, Elangovan, and Hartvigsen 1996).

3.4 Interconnect/Bipolar Plate

In the planar design, the bipolar plate connects the anode of one cell to the cathode of an adjoining fuel cell in a stack. The main purpose of an interconnect or the bipolar plate is to separate and distribute the fuel and oxidant gases to the electrodes. The desirable characteristics of an interconnect include similar thermal expansion properties, mechanical strength, and impermeable to gas to prevent direct chemical combustion of the fuel, while maintaining chemical compatibility with other cell components. In addition, it must be stable over the entire range of operating oxygen partial pressure and have high electronic conductivity in air and fuel, while exhibiting no oxygen ion conductivity.

Ceramic and metal interconnects have been investigated. Some metals have been used because of their machinability and thermal transfer characteristics; however, some of the metals being used, such as Inconel, may be cost prohibitive in the long term. Some companies, such as SOFCo¹, are studying ceramics and metal interconnect materials (Khandkar, Elangovan, and Hartvigsen 1996).

3.5 Stressor-Degradation Failure

Table 1 illustrates a stressor-degradation-failure approach applied to a typical solid oxide fuel cell. The approach developed at PNNL provides a systematic procedure for characterization of degradation properties. The procedure involves the following progressive steps

- Failure modes (symptoms detected)
- Degradation mechanism (cause of the symptom)
- Degradation stressor (activation agent behind the cause)
- Detection method (suggestions on how to measure the stressor)

The approach attempts to provide the user with a strategy for targeting the stressor that is responsible for the activation of the offending degradation mechanism; thereby getting to the root cause of the symptoms identified and systematically eliminating the failure modes.

¹ A company located in Salt Lake City, Utah that is a wholly owned subsidiary of McDermott International.

Table 1. Mode – Mechanism – Stressor Relationships

Component Part	Failure Modes [visual symptoms] What broke and in what manner?	Degradation Mechanisms [What caused the damage] What made it break?	Degradation Stressors [mechanism activation agents] What activated the degradation?	Mechanism and Stressor Detection Methods What should be measured?
Solid Oxide Fuel Cells				
Electrolyte	Cracked, warpage/bowing surface fractures	High thermal stress, reduced strength of material	Thermal coefficient mismatch with another material, deleterious material interactions	Elongation/strain of materials, temperature (T) profiling, acoustic emission (AE) of components
	Cracked, warpage/bowing surface fractures Cracked warpage/bowing surface fractures	Mechanical stress (materials are not flat) High stress	Pressure too high on cell stack or material is too brittle Sealing material contacted electrolyte	Measure force on stack and response (strain/deflection) of cell component, material properties Viscosity of sealing material, T profile, microstructure of electrolyte, AE of components
Cathode	Low power output, degrading performance	High activation polarization.	Low O ₂ activity/pressure at site	p(O ₂) at interface, gas chromatography (GC) or p(O ₂) sensor, impedance spectroscopy (IS)
Anode	Low power output, degrading performance	High activation polarization.	Low fuel activity, low pressure at site	p (fuel) at interface, GC, T profile
	Low power output, degrading performance	High concentration polarization	Fuel leaks/reactants not making it to the site	Fuel utilization, differential pressure (dp) of fuel and O ₂ , T profile, IS
Interface	Cracking	Heat gradient	Fuel leaks/fuel took alternate path or obstructed	Thermal profile across the cell, volumetric check of exhaust gases, fuel flow balance
Interconnect	Cracking	Heat gradient at the interface	Fuel took alternate path or the path is obstructed.	Thermal profile across the cell; fuel flow balance

4.0 Review of SOFC Programs

4.1 Objectives

The following paragraphs contain a brief summary of worldwide investigative efforts in the SOFC technology. An attempt has been made to include the major manufacturers and researchers involved at this time (October 2001) in SOFC technology. Major programs and their achievements are noted to baseline the progress in this technology.

Many programs are being sponsored throughout the world in solid oxide fuel cells. In the United States, many organizations are studying planar SOFC designs, including Honeywell, Ztek, McDermott, Technology Management, and Ceramatec. Some of these developers are part of a new program called Solid State Energy Conversion Alliance (SECA). The program, led by two national laboratories, PNNL and the National Energy Technology Laboratory (NETL), was formed to develop solid-state fuel cells. Based on a 5-kW low cost, high power density, modular design, the plan is to mass customize and build units for multiple applications. By the year 2010, a low cost unit (\$400/kW) in the multi-kW range is planned and after that is a success, a smaller unit, at an even lower cost (\$50/kW) for transportation applications, will be marketed.

The European Commission (EC) provides a small amount of funding for fuel cell development, with major funding coming from industrial organizations. However, the fact that an EC project typically involves several partners from different European Union (EU) states facilitates information exchange and collaboration efforts. Companies, such as Siemens (Germany), Bertin Technologies (France), Riso National Laboratory (Denmark), CERAM Research (United Kingdom), Rolls Royce (United Kingdom), and GASTEC (Netherlands) are involved in these projects.

The EC programs have concentrated on stationary fuel cells for heat and power applications and on mobile fuel cells for transportation. The program for the years 1994-1998 had three complementary parts, JOULE, THERMIE, and BRITE-EURAM, which focused on basic fuel cell stack and system research, economic feasibility of innovative technologies, and production process, respectively. Since 1999, European research has focused on planar stacks from 5 to 20 kWe and the design of a new SOFC product in the 200- to 500-kWe power range. In 2000, a demonstration project began to test a SOFC/gas turbine in the MW class, based on tubular SOFC technology (Lequeux 2001).

Other than these major programs, many other groups have industrial sponsors. The following sections list those programs, outlined by type of SOFC design.

4.2 Tubular Versus Planar Designs

Siemens Westinghouse (previously Westinghouse Electric) has been researching SOFC technology for more than 20 years (Appleby 1996) and is in the final stages of a tubular SOFC design development program. At this stage in the program, they are focusing on cost reductions, scale-up, and demonstrations of commercial units at customer sites.

Other companies, such as Mitsubishi Heavy Industries, also have been working on tubular designs, but Siemens Westinghouse is the recognized leader in this technology. The tubular SOFC technology was pursued, in part, because the ceramic tube technology (extrusion, attaching, sintering, and coating) was proven and available.

Likewise, production methods for planar designs will need to be as well developed for comparable progress to take place. In addition to the production advantages, tubular design was adopted because of the problems associated with sealing cells and joining multiple cells. Despite these issues, planar fuel cells have several advantages over the tubular design. The flat planar structure does not have the long current path, thus lower resistance (as opposed to tubular design) leads to enhanced volumetric power density. These high power densities make planar design more feasible for certain applications, in which space is limited, such as transportation. Moreover, lower cost fabrication methods, such as tape casting and screen-printing, can be used for planar designs to introduce cost benefits. However, the ability to scale-up and economically produce cells with some of these techniques has yet to be proven.

4.3 Combination Design Approach

Rolls-Royce Strategic Research Centre has developed a SOFC design they believe is a combination of the tubular and planar designs. Their Integrated Planar Solid Oxide Fuel Cell (IP-SOFC) design expects to capitalize on the low cost components, the short current paths giving low cell resistance and high power density of the planar, and unconstrained thermal expansion of the tubular design (Gardner et al. 1999). Fabrication of the key component of the IP-SOFC, the "multi-cell membrane electrode assembly (multi-cell MEA) module" has been successful. The component carries many series-connected cells with supported electrolyte membranes only 10- to 20- μm thick (so lower temperature operation is possible). They use ceramic interconnects, and a thick electrolyte design. In addition, the wet slurry printing approach was adopted for fabrication. The IP-SOFC design includes a housing that serves as a manifold for the fuel gas, and a unique sealing arrangement; the cells are connected by an interconnector fabricated onto the cell housing (Larminie and Dicks 2000).

Rolls Royce is working on a number of SOFC projects, including a joint effort sponsored by the EU and led by Riso National Laboratory. This project (Low Cost Fabrication-SOFC or LOCO-SOFC) is focusing on low cost fabrication and improved performance of SOFC operating at higher temperatures (over 800 to 1000°C). The IP-SOFC project is planning to reduce the stack costs to \$300/kW, generally believed to be the commercial target for widespread introduction of SOFC (Gardner et al. 1999). Recently, Rolls Royce has joined an agreement to lead an Integrated Modeling SOFC Gas Turbine

program to develop the capability to assess the performance of fuel cell/gas turbine hybrids and a multifunction SOFC program to develop a 20-kW atmospheric modular stack system (Lequeux 2001).

4.4 Planar Design

In the planar SOFC technology field, Siemens has studied MEAs (membrane electrode assemblies), defined as electrode-coated electrolytes. The MEAs are arranged in units on big bipolar plates in multiple array stacks. A 10-kW cell was successfully tested, and a new program began with a goal to develop a 50-kW plant. They developed a test stand and examined BOP issues, such as fuel preparation (i.e., removal of sulfur), air supply heat exchanger for heat recuperation, and transformation of direct current to alternating current (ac). However, Siemens terminated the project in February 1999 to concentrate on their more advanced tubular design (Lequeux 2001).

Sulzer Hexis Ltd. is sponsored primarily by industrial partners. In 1991, they began developing SOFC systems for decentralized heating and heat generation for households. They have many utility partners including Tokyo Gas (Japan) and Thyssen Gas (Germany). They have four units that have been running on natural gas, output of between 1 and 1.5 kWe, and an electrical efficiency of between 30 and 35 percent. At the same time, they have been working on system integration issues for commercialization of a 1-kWe system. Since February 2000, a 1-kW field unit has been operating at Fundamental Technology Laboratory of Tokyo Gas Company (Yasuda 2001). Their design includes one cell per planar surface, metallic interconnects, and a thick electrolyte.

Alstom is working on a program for development of the SOFC for the distributed generation market. The activity is focused on planar SOFC stacks operating at less than 800°C to lower costs. The long-term goal is to develop a low cost concept for a 20-kW system (Lequeux 2001). In the short term, they are focused on a 5-kW SOFC planar stack that is anode supported to reduce the operating temperature down to the 700-800°C range. The stack will be enclosed in a stainless steel manifold and mounted in a test facility. A test facility will be designed to operate on methane and be mounted with instruments for monitoring. The plan is to run a 2000-hr performance test on this 5-kW unit (Pyke and Lequeux 2001).

SOFCo (of Salt Lake City, Utah) is a wholly owned subsidiary of McDermott International and is (along with its partner Ceramtec) considered one of the most advanced in planer solid oxide fuel cell (pSOFC) stacks in the U.S. The researchers have developed a (patented) CPn module design multi-stack fuel cell. The design features multi-stage oxidation that allows the fuel to be consumed over many stages. It is a cross flow arrangement with a maximum cell size of 20 cm by 20 cm (published to date) limited by ceramic flatness, strength, and fabrication constraints (Appleby 1996).

In addition, Ceramtec has tested a 1.4-kW module and has a limited partnership with The Babcock and Wilcox Company of Lynchburg, Virginia for the commercialization of the technology (Williams 1997).

Recently SOFCo has begun a new program, called Affordable Manufacturing of Power Systems (AMPS), to advance the manufacturing technology of SOFCs. The team consists of McDermott Technology Inc. (MTI), Ceramtec, and Advanced Refractory Technologies, Inc. (ART). MIT designs

the stack, Ceramtec develops the materials, and ART develops the manufacturing process. The initial goal is to overcome some of the materials cost issues. The approach is to integrate the SOFCo fuel cell materials technology with multilayer ceramic manufacturing technology to accomplish the following:

- reduction in process steps to lower manufacturing costs
- superior interfacial contact between the electrochemical active components that enable performance improvement
- use of established multilayer ceramic manufacturing methods with proven success in the electronics industry.

This approach includes the co-firing of stacks of cells that offers challenges as a result of the chemical and physical constraints of the materials to produce flat, defect free, functional cells. They have fabricated flat, 10-cm by 10-cm cells with minimal warpage. This program has successfully demonstrated a co-firing process for pSOFC (Elangovan et al. 2001).

The Ztek Inc. of Waltham, Massachusetts has developed and tested a circular stack. The system consists of internally manifolded bipolar plates and electrochemically active layers with internal seals. It includes an option that allows insertion of internal reforming plates. The bipolar plates are corrosion resistant and conducting, which seal by mechanically spring loading in tension against the electrochemically active layers that are held in radial compression. This module was developed for 100 MW to 1 MW applications. By 1994, they had operated a 15-cm diameter, 10-cell stack that delivered 0.1 kW. A 25-kW version is under development at Foster Wheeler Development Center, Livingston, New Jersey with an expected 63 to 68 percent lower heating value (LHV) efficiency in a co-generation application system (Appleby 1996).

The Interscience Radial Flow (IRF) SOFC was developed in 1980 and acquired by Technology Management Inc. (TMI) of Cleveland, Ohio. It is reportedly similar to the Ztek system with internal manifolding via holes and outward radial co-flow of reactant gases in each cell. It uses metal bipolar plates. One unique feature of the system is the use of particulate, rather than sintered, air electrodes, which were developed to replace the matched thermal expansion coefficient.

PNNL (in Richland, Washington) is developing technologies in several areas of SOFC. PNNL is studying the microstructure of the anode and cathode to improve the performance of the electrode materials. Various materials and manufacturing technologies, including advanced sintering techniques, have been studied. Progress has been made in fabrication and testing of prototypes for single and multiple cell stacks and in the optimization of reformation processes of hydrocarbons integrated with the cell stack. In addition, cost effective, and reliable sealing material and interconnects are being developed. In parallel with this work, stress thermomechanical and thermal-fluids modeling are also being conducted to complement the experimental work. Currently, the focus is to achieve higher stack power density, the ability to handle thermal cycles, hydrocarbon reformation process on the cell or integrated with the cell stack, and lower cost (Singhal 2001).

At the University of Missouri-Rolla (UMR) tests have demonstrated compositions that would air sinter below 1500°C to 95 percent of theoretical density. They also have illustrated the use of a spin-coating technique that can produce a thin, dense layer of YSZ on LSM at low temperatures and the use of a buffer coating between LSCF ($\text{La}_{0.6}\text{Sr}_{0.4}\text{Co}_{0.2}\text{Fe}_{0.8}\text{O}$) and YSZ to eliminate high temperature interactions during sintering. The UMR also collaborated with Penn State University on development of a new cathode material (Appleby 1996).

In 1985, Argonne National Laboratory (ANL) (Chicago, Illinois) invented the monolithic SOFC concept. The technology was transferred to Allied Signal Corporation. The focus is now on vertical and horizontal scale-up and operation at 800°C. The use of dip-coating to prepare thin component films has enabled excellent performance at 800°C (1.3 A/cm², at 0.9 V at low utilization). ANL has developed a borate glass-ceramic seal to avoid the interaction of silicates with SOFC components and a new Ni-Fe alloy for bipolar plates, which has a coefficient of expansion matching YSZ. Currently, ANL is promoting a test facility they developed for performance evaluation of low temperature proton exchange membrane (PEM) cells in the range of about 100 W to 250 kW.

A modified design of the monolithic structure has been jointly developed by the Chubu Electric Power Company Inc. (CEPCO) and Mitsubishi Heavy Industries Ltd. (MHI). The Mono Block Layer Built (MOLB) design has several advantages, including small space requirements and high power density. In 1996, a power output of 5.1 kW was recorded on 200 mm by 200 mm 40-cell two stacks, followed by the development of 10 kW modules in 1997 (Sakaki et al. 2001). Several of these 10-kW units were tested in 2000. Tests are now being conducted on a new T-MOLB type SOFC. Very stable operation has been noted at 15 kW. The test period has reached 3000 hours.

Honeywell (formerly Allied Signal of Torrance, California) has developed a flat planar solid oxide fuel cell that utilizes a thin electrolyte with a relatively thick anode. The cell is designed to operate at reduced temperatures, between 600 and 800°C. Numerous stacks have been constructed and power densities of over 650 W/cm² at 800°C have been demonstrated. Single cell work is focusing on increasing power densities, improving flatness, evaluating sulfur effects, and establishing performances on syngas. Work is proceeding on modifying stack design, (gas manifold) interconnect materials, and establishing stack performance parameters.

Since 1992, Ceramic Fuel Cells (CFCL) has grown to include a large focused program for development of ceramic pSOFC technology. They have achieved a significant intellectual property position in know-how and patents, with over 80 people and \$60 million invested in the venture (Godfrey et al. 2000). The CFCL focus is on tape casting and screen-printing of electrolyte-supported cells. They use stainless steel (sheet metal) interconnect material with novel attachment methods that are predicted to lower cost and extend the life of the cell. In addition, they are developing sealing technologies for a variety of different designs and temperatures. Accomplishments include testing a 4 by 2 array, 50-layer stack that utilized the steel interconnected electrolyte-supported cells and producing a 5.5-kW output. It has operated for approximately 400 hrs and generated 720 kWh of power. Moreover, they constructed a 22-layer, 2 by 2 array stack, anode-supported cell that operated at 760°C. It prematurely failed (producing only 2.7 kW for 20 min.), but showed good stability and minimal degradation effects.

CFCL has established state-of-the-art facilities for planar SOFC R&D that include 20 test stations with diagnostics to test single cells and stacks of cells up to 5 kW. In May 2000, they tested a 25-kW experimental test bed facility. However, the complete system was never demonstrated, due to stack failure problems including excessive leaks at the fuel inlet manifold caused by thermal expansion differences in materials and production problems. Their future plans are to expand the facility and scale-up to demonstrate pilot manufacturing capabilities. The goal is to achieve commercial introduction of market-entry products in 2002.

5.0 International Energy Agency Collaboration Efforts

5.1 Introduction

An international collaboration, The International Energy Agency (IEA), was established in November 1974 to initiate cooperation among a number of industrialized countries. Currently, 25 countries are represented, with the Commission of European Communities also participating. The IEA program to advance fuel cells was established in April 1990, and included five annexes: Annex I Molten Carbonate Fuel Cell (MCFC) Balance of Plant Analyses, Annex II: Solid Oxide Fuel Cells, Annex III: Carbonate Fuel Cell Materials and Electrochemistry, Annex IV: Polymer Electrolyte Fuel Cell (PEFC), and Annex V: Systems Analysis.

ANNEX II of the SOFC system is multifaceted, covering issues such as evaluating modeling techniques, recommending test procedures and reviewing system stack design requirements. Many of these Annex II activities were reviewed, and one of special interest to this report was called Subtask B: Recommended Practices and SOFC Products Evaluation. The following items were focused on during the review of Subtask B:

- B1: Long-term stability in operating condition
- B2: Thermomechanical evaluation
- B3: Sample and data bank
- B4: Stack evaluation from systems
- B5: Instrumentation and diagnostics
- B6: Patent search.

Tasks B2 and B5 will be reviewed in more detail.

5.2 Thermomechanical Evaluation (Task B2)

The Thermomechanical Evaluation task was defined as a method to provide useful tools to ceramic material researchers involved in SOFC technology (specifically flat SOFC configurations expected to operate at temperatures in the 600 to 950°C range). These tools were designed to facilitate studying and comparing a variety of thermomechanical quantities in different laboratories¹. The recommended practices, listed in an IEA document, typically do not require any highly sophisticated instrumentation to address the need of rapid, economical, easy to handle methodology for characterizing the specimens under preparation. They often refer to accepted standards, list a single method per parameter, refer to *as-fired* or *as-sintered* specimens and, unless otherwise stated, suggest room temperature tests. The

¹ IEA publication (not publicly available). H. Nabilek. 1997. "SOFC Research in international cooperation: The IEA SOFC Annex." 97-18, pp. 26-34. eds. H. Nabilek and A. McEvoy, (KFA-IEA) Research Centre Julich-International Energy Agency, Julich, Germany.

following list provides parameters that were developed for this task and deemed to have a significant impact on the operation and life cycle of the fuel cell.

- Geometrical factors: thickness, warpage, roughness
- Elastic properties: Young's modulus, shear modulus, Poisson's ratio
- Mechanical properties: biaxial flexure, strength, toughness
- Physical properties: porosity, density
- Thermal properties: thermal cycling, thermal expansion, thermal diffusivity/conductivity. (Note: Thermal expansion and thermal diffusivity were still under revision (as of the SOFC V 1997 publication) at the time this report was prepared.

Other parameters that still need development are material degradation, crack propagation, and emissivity. For example, the study of degradation (by IEA) has revealed no systematic procedures available for characterization of degradation properties. The study did discover the following:

- Interface degradation is more serious than the bulk
- Anode degradation is generally larger than cathode degradation
- Little information is available about the seal, interconnect, or electrolyte degradation.

This IEA task group also recognized the need for liaison with the International Standards Organization (ISO).

5.3 Instrumentation and Diagnostics (Task B5)

The Instrumentation and Diagnostics task was to develop methods that would be applicable to R&D and future practical applications. Initially, the IEA participants agreed on laboratory procedures to standardize recognized practices for measuring some basic parameters, such as current, voltage, gas flows, temperatures, pressures and compositions, and power output. In addition, electrical methods including ac and high frequency (hf) techniques (such as impedance spectroscopy) were accepted as methods that can be used to understand electrochemical effects at interfaces, grain boundary, and bulk effects in the electrolyte¹.

Before choosing an approach, the vital parameters for safe and proper operation of a SOFC system must be determined and the constraints for such instrumentation as a result of the limited access, high temperature and heavily insulated enclosure, must be considered. An appropriate range of diagnostic tools, as well as data acquisition and analysis equipment, could then be identified and adopted.

Realizing the constraints, several innovative techniques were reviewed to complement the standard practices. Temperature and stress measurement with metallic thin film devices and non-contact optical choices were considered, yet proved unfeasible because of material problems.

¹ IEA publication (not publicly available). A.J. McEvoy. 1996. Instrumentation and In-Situ Diagnostics: Final Report of Activity B5. (KFA-IEA) Research Centre Julich-International Energy Agency, Julich, Germany.

Optical techniques have advantages and disadvantages. Fiber optics for gas analysis (with gas absorption spectra) was acknowledged. Also, zirconia is (in principle) transparent, appearing white and opaque because of scattering processes. Therefore, incorporation of color centers, such as 4f ions, could indicate by fluorescence the short-range structural environment in which those probe ions are found¹. The high temperature environment, in which the thermal radiative emission in the IR is visible, is so strong that it is difficult to obtain accurate optical readings.

The measurements of acoustic noise with piezoelectric transducers to detect cracking and ultrasonic detection of interconnect-cathode integrity in stacks were offered as potential options. In one particular case in which methane was the fuel, a high level of electrical noise was observed and showed correlations with the functionality of the anode.

¹ IEA publication (not publicly available). . A.J. McEvoy. 1996. *Instrumentation and In-Situ Diagnostics: Final Report of Activity B5*. (KFA-IEA) Research Centre Julich-International Energy Agency, Julich, Germany.

6.0 Research Listed by Key Parameters of SOFC Efficiency

6.1 Evaluation and Testing of Voltage Losses

Some techniques that are well established in aqueous electrochemistry are adapted to solid electrolyte cells, such as in SOFC. However, how well they are being applied is still being debated. Some of these methods include:

1. Impedance spectroscopy (IS) is a technique to characterize the kinetics of an electrode-electrolyte interface. Two main methods are used to measure impedance, time domain and frequency domain techniques. The frequency domain technique, often used in SOFC experiments, typically involves a potentiostat and a frequency response analyzer. The electrochemical potential of a working electrode (the one under investigation) is modulated sinusoidally with respect to the reference electrode. The response of the current is monitored and by division of the harmonic part of the potential and the harmonic part of the current, the impedance can be calculated. The impedance is a frequency dependent complex number that can be plotted in a variety of ways, but is generally plotted in the complex plane. By fitting this impedance spectrum to a model or an equivalent circuit, an equivalent circuit for the system can be obtained (Condensed Matter Department of Universiteit Utrecht 2001).
2. The current interrupt method is typically applied to single cells and small stacks and involves a cell that is operating and generating a current at which the concentration polarization is negligible. Thus, the voltage drop will be caused by the ohmic and activation losses. To apply the method, the current is suddenly shut off, so the charge double layer and the associated activation overvoltage (V_a) will rise slowly back to OCV, while the voltage (V_r) drop caused by the ohmic losses will immediately rise. The graph of voltage versus time in Figure 4 shows a typical response to the method (Larminie and Dicks 2000).

Many researchers have applied the current interrupt method or impedance spectroscopy in many SOFC evaluations. Van Herle and Thampi¹ have experience testing with reference electrodes and share some of the potential problems and how to avoid them. In a single SOFC application, the losses (disregarding losses such as current collectors, leaking) of one positive electrolyte negative (PEN) are broken down into:

- cathodic non-ohmic overpotential, η_c
- electrolyte ohmic losses, R_e
- anodic non-ohmic overpotential, η_a .

¹ IEA publication (not publicly available). . J. Van Herle and R. K. Thampi. 1996. "A remark on the use of reference electrode in SOFC testing." pp. 26-31, eds. H. Nabeelek and A. McEvoy. (KFA-IEA) Research Centre Julich-International Energy Agency, Julich, Germany.

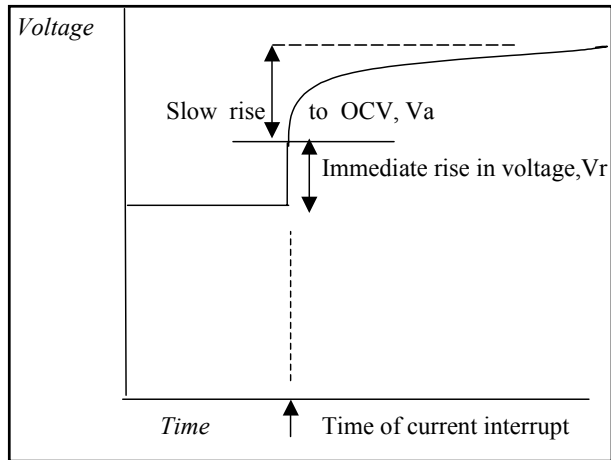


Figure 4. Current Interrupt Method Applied to a Fuel Cell

According to this research, the electrolyte ohmic loss can be determined by the current interrupt technique or impedance spectroscopy without the help of a reference electrode (that is, by summing both overpotentials). However, to determine the overpotential of either the cathode or the anode, a reference electrode (RE) is required. Initially, some terms commonly found in literature and often found to be confusing are defined as:

- The potential drop measured between the cathode and RE (as current flows through the cell)
 $= \eta_c + iR_c$
- The potential drop measured between the anode and RE (as current flows through the cell)
 $= \eta_a + iR_a$
- The relationship between the losses results in $R_c + R_a = R_e$

The analysis performed by these researchers shows the values of R_c and R_a cannot be expected to equal $R_e/2$, and tests do not indicate a pattern to easily determine the location of the equipotential line (EQP) of the reference electrode. The value of either of the two terms, R_a or R_c , must be determined for each test. Further, performing the tests incorrectly leads to erroneous conclusions as to which electrode (the cathode or the anode) is the limiting factor in the cell.

A diagram from the literature¹, Figure 5, illustrates some of the variations discovered by Van Herle and Thampi² related to setting up these types of tests. The sketch depicts the placement of the reference electrode and states the reference electrode is placed on the surface of the electrolyte outside the electrode regions. The recommended distance d is suggested to be at least 10 times the electroplate thickness d_e (referred to as the $d > 10 * d_e$ rule) with a minimum distance for d given as 1 mm. The tests done by these researchers (Van Herle and Thampi) display that the minimum distance for d should be 3 mm (rather than 1 mm), and they believe the $d > 10 * d_e$ rule is exaggerated.

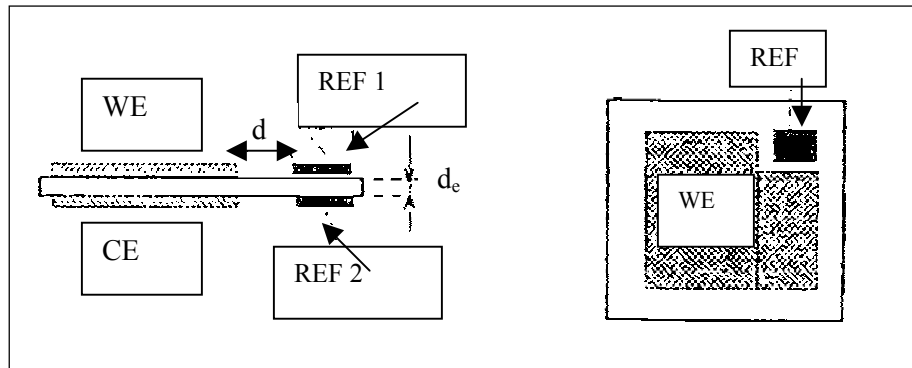


Figure 5. Typical Reference Electrode Test Set-Up

As stated by Van Herle and Thampi, the equipotential line can be determined by measuring the ohmic drop between the RE of either of the electrodes. A correct procedure, according to these researchers, is depicted in Figure 6.

Curve 1 depicts the cell operating normally. Curve 2 and Curve 3 are the voltages between the cathode and the RE, and the anode and the RE, respectively, recorded while drawing the same normal current through the cell as depicted in Curve 1. To do this, five lead wires are needed, three different V-I curves are obtained and the same maximum current i_{sc} (short circuit current) can be found with all three curves. The ohmic voltage drops R_c and R_a can be measured by impedance spectroscopy and subtracted from Curves 2 (cathode overpotential) and 3 (anode overpotential) to give the true overpotential for the cathode and anode.

¹ IEA publication (not publicly available). Bern, C. 1992. *Recommended Practices for SOFC Products*.

² IEA publication (not publicly available). J. Van Herle and R. K. Thampi. 1996. "A remark on the use of reference electrode in SOFC testing." pp. 26-31, eds. H. Nabelek and A. McEvoy. (KFA-IEA) Research Centre Julich-International Energy Agency, Julich, Germany.

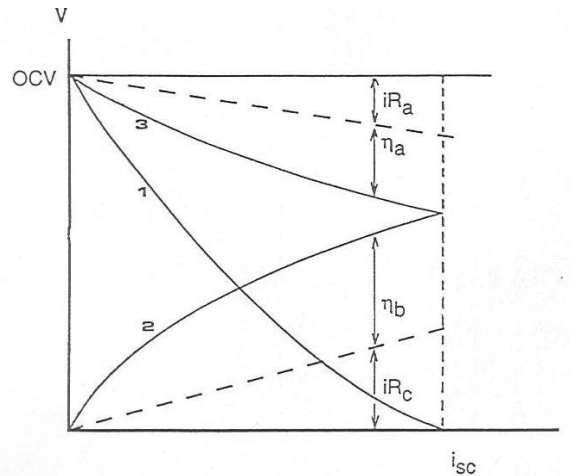


Figure 6. Sketch of Procedure for Deriving Overpotential Curves

Other caveats to IS are noted in the literature (Edwards et al. 1997), specifically when using the three-point (or four-point) spectra technique commonly applied to SOFC. The advantage of applying IS to SOFC is to be able to define the electrical responses of the different microstructural regions in the fuel cell. It becomes possible to define not only the overall bulk regions, but also the grain boundaries within a sample. The challenge is to identify which IS feature corresponds to which element of the microstructure. Correct interpretation relies on obtaining accurate impedance data over a wide frequency range. This process can be complex and lead to errors caused by many factors, such as:

- instrumentation limitations: Impedances associated with the equipment, such as leads, cables, and sample holder that are not accounted for.
- complications between the sample impedances: The electrical responses of the highly active (low polarization resistance) electrodes becoming convoluted with the response of the low conductivity electrolytes.
- reference electrode itself often has very high impedance, causing a significant voltage drop that needs to be considered.

The researchers cite several possible ways to minimize these errors in testing, and obtain accurate repeatable results.

According to Virkar et al. (1999), two basic designs are being explored in the development of the SOFC. They have evaluated the advantages and disadvantages of these designs, based on electrochemical techniques. The designs that were studied are:

1. The electrolyte-supported design in which the electrolyte is the thickest component ($\geq 150 \mu\text{m}$) and provides the support, with electrodes silkscreen printed on it. In this case, the electrolyte ohmic

contribution is large because of the high electrolyte resistance. For this reason, these cells are being developed for $>1000^{\circ}\text{C}$ temperatures, where the electrolyte resistance is low (typically 20 ohm/cm).

2. The electrode-supported design in which one of the electrodes, cathode or anode, is the thickest and provides the support. In this case, a 30- to 40- μm layer of YSZ is deposited on a porous LSM cathode (of 2-mm thickness) or in the case of the anode, an YSZ layer (of 10 to 20 μm) is deposited on a relatively thick Ni+YSZ anode.

The overall performance of these cells is dictated by various polarizations (ohmic, activation, and concentration).

YSZ is the most widely used electrolyte because of its excellent stability in both reducing and oxidizing environments, even though its conductivity is lower (resistance is higher) than other materials.

At 800°C , the resistance of YSZ is about 50 ohm/cm, which translates into an area specific resistance (electrolyte contribution) of about 0.75 ohm per cm^2 . This value is very high and results in a power density that is low at temperatures below 950°C . However, in electrode-supported cells, the YSZ electrolyte thickness need be only 10 μm . A 10- μm electrolyte has an area specific resistance of 0.05 ohm cm^2 at 800°C . However, despite the low ohmic contribution, the area specific resistance of the cell as a whole may be several times higher because the activation and concentration polarization can outweigh the ohmic contribution.

Activation polarization is related to charge transfer processes and, thus, depends on the nature of the electrode-electrolyte interfaces. Concentration polarization is related to transport of gaseous species through porous electrodes and thus is related to the microstructure of the electrodes, specifically the volume percent porosity, the pore size, and the tortuosity factor.

This study indicated the principal losses in SOFC are attributed to the activation and concentration polarizations when the electrolyte is thin. This design, a thin electrolyte supported by an electrode, can result in very acceptable output; power densities of 1.9 ohm/ cm^2 at 800°C were recorded. Another conclusion was that one manner of reducing the activation polarization (on the cathode side) is by using a composite electrode. For example, an electro-catalyst like LSM and an oxygen ion conductor like YSZ could be used to spread the reaction zone distance into the electrode and make the electrolyte-electrode interface a more diffuse interface.

Another evaluation performed by Ringuede, Fouletier and Dessemond (2000) involved testing of SOFC cathodes using impedance spectroscopy. Specifically, IS was used to characterize the kinetics of the electrode-electrolyte interface and the influence of the current collecting on single graded electrodes - (mixtures of YSZ and LSM) and on double graded electrodes (mixtures of YSZ and LSM and mixtures of LSM and strontium doped lanthanum cobaltite, LSCo) deposited on 150- μm thick YSZ films. The evaluation was to determine how the quality of the current collector could alter the performance of the electrodes and electrolyte.

The impedance spectroscopy measurements were carried out under open current voltage conditions, during heating and cooling cycles. The electrolyte response was broken into two semicircles, for high (hf) and low (lf) frequency responses. The electrodes response was one to three overlapping semicircles. However, the focus of this work was the polarization resistance (R_n).

The collectors tested were sputtered silver, silver paste, and platinum grid. The results indicated that the electrolyte resistance was not altered by the nature of the current collector; therefore, a homogeneous current density distribution within the electrolyte can be assumed. However, the polarization resistance (R_n) was very dependent on the type of current collector, even when LSCo was used. It was also observed that lowest R_n values were recorded with sputtered silver and the highest with platinum grid. Further, the degradation of the electrode performance was considered to be caused by the loss of contact area on the outer surface of the electrode. Some of this effect was attributed to the sputtered current collector being applied so that it matched the outer surface of the electrode, while the metallic grid only made point contact on the surface. As such, the metallic grid type current collector displayed reproducible values of polarization resistances for both materials tested.

A different group (Guillodo, Vernoux, and Fouletier 2000) studied current collectors and discovered some interesting facts. They evaluated the changes in electrochemical behavior of electrodes as a result of using different types of current collectors.

The two types of current collectors that are commonly used are paste and mesh. The paste is coated onto the electrode material, specifying fairly accurately the contact area. The mesh acts like a mimic of the interconnect material.

A variety of current collector material was tested using impedance spectroscopy (IS) at open circuit voltage in hydrogen and water (H_2 - H_2O) atmosphere at $800^\circ C$ using a symmetrical cell. A perforated alumina cell was used with the sample introduced into the cell and heated for 5 hours. The working atmosphere was hydrogen, argon, and steam, controlled by mass flow meters at a controlled temperature to set the water vapor partial pressure. Gas compositions were measured in volume percent. The impedance measurements were done in the 10^4 to 10^{-3} Hz frequency domain.

The four current collectors tested were gold paste, platinum paste, nickel paste, and nickel mesh. The tests indicated that the paste current collectors resulted in similar ohmic drops, while the nickel mesh had a significantly higher ohmic drop. The overall ohmic resistance that included the resistance of the electrolyte, electrodes, and the contact resistance between the electrodes and the current collectors, was higher than the electrolyte resistance by itself. Moreover, when using the paste, the polarization resistances were in the following order: $Ni < Pt < Au$. It was also observed that polarization resistances for all the paste applications increased with time, generally as a result of metal particle diffusion through the Ni-YSZ cermet. This result demonstrates that the paste current collectors interfere with the electrochemical properties of the anode material.

Using nickel mesh, the electrochemical properties did not change with time. Based on the electrochemical study of Ni-YSZ cermet in H_2 - H_2O atmosphere, the researchers concluded that nickel mesh was the best current collector (Guillodo, Vernoux, and Fouletier 2000).

6.2 Evaluation and Testing of Reactant Utilization

Although the way the fuel is utilized is more often a concern and is the focus of the fuel efficiency definition, it is also important for the oxygen to be utilized appropriately. Thus, a more general discussion of reactant utilization and associated testing for losses is included in this section.

The OCV is often used to detect seal leaks. Leakage of air into the anode stream reduces the fuel utilization while producing no current, and reduces the reversible potential because of loss of hydrogen activity. The reaction will also increase the steam activity, thus lowering the operating voltage. In this way, OCV can be a measure of seal effectiveness.

In a planar configuration using pressured air to force oxygen into the cell, air leakage into the fuel streams will often occur along the air inlet side of the cell. The fuel channel closest to this air channel is most affected by the air leak, and the reversible potential near the fuel exit (of this outside channel) is lower than the fuel inlet of a center channel. Therefore, under operating conditions, air leakage results in reduced current density near the air inlet face and loss of efficiency by non-current producing fuel consumption (Hartvigsen et al. 1996).

Another complication is the mixed conductivity of the interconnect material. Ideally, the interconnect is only an electronic conductor, but the material most often chosen (LSC) has depicted some ionic oxygen conductivity at operating conditions. The exact degree of oxygen conductivity will be dependent on the characteristics of the material (dopant scheme), the operating temperature, and the oxygen potential on each side of the material. This process leads to fuel being consumed electrochemically, but the current produced is shorted back through the interconnect.

To evaluate the effect of non-uniform cell potential, two identical single cells were set up, with one test bed set-up using RT humidified hydrogen. The other test bed had the same set-up with an additional stream of controlled oxygen that could be *leaked* into the fuel stream. The fuel supply can be individually controlled for each test set-up and the OCV can be individually measured or connected in parallel. The parallel operation simulates a single cell in a stack with a non-uniform reversible potential and an imposed electrical isopotential that induces an internal current loop.

The air to fuel ratio was varied in small increments, and the cell voltages were measured individually with parallel connections. The results indicated that stack OCV is more indicative of the lowest reversible potential on the cell than the reversible potential of the cell average fuel composition.

Some of the attempted test methods worked while others did not. One of test beds used an *in-situ* oxygen sensor that displayed favorable results when compared to other research results obtained. One of the test beds attempted to condense all the water out of the fuel to check oxygen content. This method yielded impractical results (that is, less oxygen was measured using this technique than the first method, which raised questions such as whether all the water was condensed out of the fuel.)

The oxygen conductivity on the LSC film was reduced by adding steam (thereby increasing the oxygen activity in the fuel stream). However, this was only done as a diagnostic tool and would not be advisable for use in an actual cell because of the reduction in stack performance. Other interconnect material was used and compared against the LSC material. (This latter material is not suitable for long-term, but all right for <100 hrs, and was only used to eliminate the possibility of oxygen transport through the material.) This part of the experiment showed that, by reducing or eliminating ionic conduction in the interconnect material, high fuel utilization and higher efficiency is possible (Hartvigsen et al. 1996).

Mogensen et al. (1999) from the Riso National Lab in Denmark, described some of their experiences with the electrochemical performance of the SOFC. It is stated up front that three types of cell tests are involved and each type of test has a different purpose and, thus, different associated procedures and outcomes. The three tests are:

1. Quick test: This test is interested in relative results only (that is, did the change improve performance?). Therefore, measure and analyze only a few parameters, such as I-V curves, generally done with low concentration of H₂ so safety issues are at a minimum.
2. Comparison test: This test is to compare the quality of a cell with the results of other cells; thus the goal is to minimize the importance of the test procedures as much as possible or, at a minimum, quantify the effects of differences between test procedures.
3. Full comprehensive test: This test is to demonstrate operational performance (such as durability, economic feasibility) under specific circumstances to prove future commercial success.

The latter involves many hours of testing under different operating conditions, thus is more expensive and complex. Therefore, the goal is to perform less expensive tests, and relate the outcome of these tests to the more complex and expensive versions. To achieve this, many developers are trying to pick one or two key parameters that will indicate the overall performance of a fuel cell. This parameter is often power density, yet it is too dependent on fuel composition and cell polarization. Thus, area specific resistance (ASR) in ohm/cm² is a better choice. It has no accepted definition, but it is agreed that it is less dependent on test circumstances than power density. The definition used in this test is:

$$ASR = (EMF - U) / I_d$$

where EMF = electromotive force of the inlet fuel and air, U = cell voltage at the current density and I_d = design point, such as 0.6 V at 1000°C, a fuel utilization of 85 percent and an air flow of four times the stoichiometric amount of air (or 85 percent/4 = 21 percent oxygen utilization as measured at air inlet).

Overall the ASR can be divided into R_s (ohmic resistance) and R_p (electrode polarization resistance), further divided into:

$$ASR = R_e + R_c + R_{p, act} + R_{p, dif} + R_{p, con}$$

where R_e = calculated electrolyte resistance, $R_c = R_s - R_e$ resistance caused by non-optimized contacting and current collection, $R_{p, act}$ = activation polarization from processes on the electrode surface and in the bulk material and the electrode-electrolyte interface, $R_{p, dif}$ = is the contribution from the gas phase diffusion, and $R_{p, con}$ = contribution resulting from gas conversion (that is, fuel and air utilization). This break down of the resistances is based on what can be measured or calculated, not on any physical or electrochemical theory. The individual contributions of these parameters were determined and a correction factor for fuel, based on the type of flow utilized (turbulent or plug flow), was calculated. These calculated values were verified experimentally.

Tests were performed with two different set-ups. One set-up was for cells ranging from 6 to 10 cm², and designed for easy change of the cell housing and the current collectors. The second set-up was made for only one size cell with the ability to change out the current collectors.

The tests measured OCV and, on one test, showed a low OCV value (lower than the calculated EMF of the inlet hydrogen) indicating that some air leaked into the anode. The air leak caused an increase in temperature because of the combustion of hydrogen. The leak and, thus the temperature increase, were suspected to be at the rim of the cell and were not detected because the temperature probe was located at the center of the cell. The increased temperature decreased the cell resistance locally. However, the leak was never proven to be a gas leak; an alternate hypothesis given was an electronic leak through the electrolyte.

Primdahl et al. (2001) did a comparison of cell resistances obtained from full cells with the sum of losses from electrode and electrolyte performed on a single cell. They discovered the cells actually performed better at lower temperatures than expected. This prompted a review of the cell resistance and its components.

To simplify a complex matter, they split out the resistances which allowed for partial breakdown of a multipart resistance. If the overall cell resistance $R_{overall}$ (defined as $EMF - V_{cell} / i_m$), where EMF is the ideal voltage (no losses), V_{cell} = voltage, and i_m = measured current. One way to divide this resistance is by the following relationship:

$$R_{overall} = R_{cell} + R_{connection} + R_{concentration}$$

where

$$R_{cell} = R_{electrolyte} + R_{anode} + R_{cathode}$$

where $R_{electrolyte}$, R_{anode} and $R_{cathode}$ measurements were derived tests of single electrodes and electrolytes and added together to get the total cell resistance R_{cell} . The measurements for R_{anode} and $R_{cathode}$ include a contribution for diffusion losses as seen in thick, dense supporting electrodes and electrodes with current collecting layers.

$$R_{\text{connection}} = R_{\text{contact}} + R_{\text{lateral}} + R_{\text{interconnect}} + R_{\text{terminals}}$$

where R_{contact} is losses caused by contact between materials, R_{lateral} is lateral (versus perpendicular losses that are usually insignificant) losses in the electrodes and current collecting structures, $R_{\text{interconnect}}$ is losses caused by resistance of interconnect layers, and $R_{\text{terminals}}$ is losses associated with current terminals that may be included, depending on position of voltage probes in the actual test.

$$R_{\text{concentration}} = R_{\text{conversion}} + R_{\text{diffusion}}$$

From an electrochemical point of view, contributions from fuel conversion, $R_{\text{conversion}}$ and diffusion in stagnant (non-turbulent) layers above the porous structures, $R_{\text{diffusion}}$ should be considered part of R_{cell} . Care must be taken to separate $R_{\text{diffusion}}$ in stagnant gas layers from the diffusion in the porous structures. In the cell test context, they are considered as part of $R_{\text{concentration}}$ relating primarily to gas composition and utilization at the selected working point.

However, after offering this approach of splitting resistance into subcomponents, Primdahl et al. (2001) suggest that the approach may be invalid because of the anisotropic nature of a loaded system. Although a fuel cell operates under load, gas conversion causes distribution of current density, decreasing in the downstream direction. Also, fuel composition gradients that arise, often resulting from leaks, may cause different driving potentials throughout the cell. Likewise, gas leaks can alter the current density and cause localized heating by combustion. They offer some ideas on improving SOFC tests.

Some of the ways to control a fuel ratio of hydrogen (H_2) and water (H_2O) in a feed line can be done by saturation/condensation at a given temperature, by evaporation of a controlled amount of liquid water at a constant rate or by direct combustion of oxygen (O_2) in hydrogen (H_2). If no leaks or cold spots are in the feed line, the saturation temperature or the flow rate in the feed line will give the intended fuel composition and EMF. However, the EMF is based on the fuel sent to the fuel cell, thus the better average condition of the cell is the measured OCV. This approach can also be helpful because it can quantify a leak and qualify whether a test is valid. If the leak is severe enough, the data may have to be discarded. If the leak is small enough, it can be treated as a change of gas composition.

The effect of leaks on cell tests may be divided into two types

1. A loss of driving potential (OCV-EMF) caused by oxygen (O_2) entering to convert hydrogen (H_2) to water (H_2O).
2. A volumetric loss of fuel affecting the fuel utilization caused by pressure gradient versus the ambient.

Depending on where the leaks occur effects how important it is to the test, and what should be done about it. A leak before the cell affects the intended fuel composition and quantity. However, a true average fuel composition may be obtained from the cell OCV. Leaks after the cell are of no concern, unless off-gas analysis (or a balance) is being carried out. Leaks in the cell or in seal areas may cause inhomogeneous gas composition over the cell even at OCV.

The effect of leaks that cause a loss of driving potential were considered. These leaks were expected to be caused by oxygen entering in the fuel cell and converting hydrogen into water. If these leaks are independent of fuel flow rate (assuming the leak is at a constant gas velocity), an estimate of the loss of fuel can be based on observed OCV deviation from expected EMF calculated by the Nernst equation.

A number of curves were devised that show, at a given feed percentage of water, the loss of hydrogen can be estimated from the OCV-EMF deviation. From the curves it can be stated that for a given loss of H₂, (say 5 percent of the feed) a 60 mV loss of driving potential is likely if the feed contains 2 percent water; however, if the feed contains 50 percent water, the loss is only 5 mV. With this knowledge, researchers could run water-lean tests, determine the leaks rates and apply those leak rates to water-rich tests.

A different option to reduce the leak problem during testing may be to establish a reducing sweep atmosphere (say 3 percent hydrogen in nitrogen outside the test chamber). This action would reduce the pH₂ (partial hydrogen) gradient to well below one order of magnitude and prevent incoming leakage of oxygen (O₂). Other testing ideas offered by Primdahl et al. (2001) include using pO₂ sensor tubes at the inlet and outlet of the cell to give detailed information on the test conditions and using gas chromatography or mass spectroscopy to detect whether leaks are occurring. If possible, a volumetric check on the feed and off gases should also indicate a leakage.

6.3 Evaluation of Temperature

Proper temperature measuring during a cell test can be a major factor in accurate results and, if done improperly, can lead to the wrong conclusions. Cells that are fairly large (or greater than a few cm²) should be measured at multiple temperature points to account for temperature gradients across the cell. It is misleading to use the furnace temperature or gas stream temperatures. Even sheathed thermocouples in contact with the cell surface may inflict a temperature rise as a result of conduction. For example, a test set-up with thermocouples (diameter = 1.5 mm) displayed a 20°C temperature rise at 1 A/cm² at 860°C (Primdahl et al. 2001). In this test, the rise in temperature occurred within the first 2 to 3 min., so a temperature correction will be necessary in most cases.

Two papers presented by Clausen and Bak (1998) discuss the possibility of using Fourier Transform Infrared Spectroscopy (FTIR) to determine the transmissive and emissive properties of hot gases. Generally, FTIR is used for non-intrusive measurements to provide information about species concentrations and gas temperatures along the line of sight in combustion systems.

In this case, the set-up that included an FTIR instrument with an internal detector, an external blackbody source, and a heated gas cell was used to measure various concentrations of carbon dioxide (CO₂, at 0.5, 10, 100 volume percent) at elevated temperatures. The stainless-steel cell designed for this work (because cells for this type of testing are not commercially available) was heated to temperatures ranging from 294 to 1273 K.

This follow-up research by Clausen and Bak (1998) attempts to verify some of the work performed in the first phase and demonstrate the applicability of Kirchhoff's law for gas in an enclosure. Kirchhoff's law of heat radiation, which relates the spectral emissivity and absorbance of a material body, has been demonstrated for a hot gas (CO₂) enclosed in a gas cell at a known temperature. The spectral emissivity of a hot gas in an enclosure is difficult to determine directly by experiment. The temperature-dependent effects of the radiative properties of the cell window materials (a sapphire window material was used) and self-absorption effects of the hot CO₂ gas have to be measured and accounted for before the spectral emissivity can be calculated. The results of the experiments indicated it is possible to measure and calculate all major radiative contributions from a hot enclosure. In addition, it is possible to separate the net gas radiance from all radiating sources, such as the heated windows, and take into account the self-absorbing effects of the gas to determine the gas temperature based on the measured radiance. Future work will be aimed at upgrading the gas cell and improving the stability of the test system (Bak and Clausen 1999).

Haag and Honegger¹ have been performing diagnostics projects for Hexis on a continuous basis. This project was performed in three separate experiments. Metallic and foam current collectors were developed that would permit penetrations for thermocouples and potential probes.

In test 1, thermocouples used were Pt/PtRh 10 percent (type S) wire 0.1 mm, insulated with Al2O₃ tube and attached with ceramic adhesive. The anode was provided with eight thermocouples and two potential probes. The cathode had five thermocouples and five potential probes. Unfortunately, the performance of the cell was low, with a maximum power output of only 40 mW/cm² because of high cathodic resistance (up to 500 mV). Because the performance of the cell was so low, the potential measurements were not examined in detail; it would not be easy to determine the dependence of the individual losses on current density at these low ranges. The test was run for 70 hrs and the five measured reference voltages remained constant while the cell voltages began to decrease continuously after 20 hrs of operation.

The dependence of cell and reference voltages on hydrogen (H₂) mass flow was evaluated and showed the reference voltages were lower in the middle of the cell, and slightly increased with rising H₂ mass flow. The cell voltages were constant across the cell radius and rose in parallel with increasing H₂ mass flow.

The cell temperature was approximately 50°C higher than the adjusted furnace temperature. The temperature on the anode side ranged from 933 to 934 and 927.5°C in the center. On the cathode side, the temperature varied by 4°C. Of the 10 thermocouples used, 9 functioned properly with 1 failing suddenly after a few hours of operation.

In test 2, a foam current collector was used with four potential probes placed through the foam into the cathode and anode sides, beside the marked references. The maximum current density was 75

¹ IEA publication. (not publicly available). R. Haag and K. Hoegger. 1995. "Hexis-diagnostics in 120 mm diameter stacks." Pp. 48-69. eds. H. Nabilek and A. McEvoy, (KFA-IEA) Research Centre Julich-International Energy Agency, Julich, Germany.

mW/cm². The slightly lower than expected electrochemical performance is attributed to cracks in the PEN caused by the potential probes that bored into the PEN after sintering the junctions during operation. The voltages at the references were not affected by the cracks and ranged between 950 and 1040 mV with total losses of 400 mV at the cathode side and 100 mV at the anode side.

Test 3 was concerned with temperature distribution measurements. Thermocouples were penetrated through the current collector, five on the anode side, five on the cathode side and two were placed in an afterburner section. On the anode side, the temperatures were all taken on the fourth PEN of a six-cell stack. The temperatures slowly decreased as the cell voltage degraded after 100 hrs. Although the thermocouples used in this test were rated for 1000°C, they were routed out of the furnace through the afterburner zone, which was too hot (well above 1000°C) and significantly shortened the life of the thermocouples.

Haag and Honegger concluded that it was important to define the location of temperature measurement more precisely. If the temperatures are measured and are a function of current density, they do not exhibit linear behavior. The temperatures first decrease with rising current density, and then they begin to increase again. This behavior is caused by superimposition of two different effects. The combustion heat decreases with increasing current density because more fuel is converted and less burned, and secondly, the reaction enthalpy and ohmic losses rise with increasing current density.

Research by Adzic, Heitor, and Santos (1997) involved the design of a thermocouple for temperature distribution measurements in solid oxide fuel cells. A theoretical model, based on mixed convective-radiative heat transfer was used to predict the thermocouple response. The proposed flat type (Pt/PtRh 13 percent, $d_{\text{hydraulic}} = 25 \mu\text{m}$, 0.000025 meter and $L/d_{\text{hyd}} \geq 120$) thermocouple was shown to be a high sensitive, low error temperature sensor, capable of satisfying the requirements for solid oxide fuel cell thermal behavior research. Thereafter, a custom-built, thin, flat-type thermocouple was used for temperature distribution measurements at the cathode side of a planar solid oxide fuel cell. The thermocouple picked up heat that was given off by radiation from the plate and by convection from the hot gas (air). The anode was subjected to force fuel flow and the cathode natural convective air flow.

A 5 cm by 5 cm SOFC plate was constructed and mounted with the cathode facing up. The cathode was exposed to natural convective air flow (1000 ml/min) at slightly above ambient pressure. The forced convective fuel flow was 620 ml/min. To place the thermocouple very close and parallel to the plate without touching it, electrical potential was established between the thermocouple and the surface, so that contact between the thermocouple and the plate was characterized by a sharp voltage jump. This procedure enabled detection of the surface with a maximum error of 5 micrometers (0.005 mm). The thermocouple was mounted on a traversing mechanism that could move vertically and horizontally (providing spatial resolution of 5 micrometers normal to the surface and 0.5 mm in both directions parallel to the surface). At each measurement, 10,000 samples were acquired and the mean temperature evaluated. A surface temperature profile was obtained for a 3-day test cycle. High temperature conditions in the range of 950 to 1200 K have been tested. The results indicated local hot spots (about 16 K above the mean surface temperature); the highest temperatures were in the higher values of X/L and

Y/L. At the positions of the cathode-anode interconnections, at $Y/L = 0.35$ and $Y/L = 0.7$, a temperature rise was present in the range of between 3 and 5 K resulting from the increased ohmic heat production.

Research by Honegger et al. (1999) demonstrated the performance of ceria-based (cerium oxide) SOFC stacks operated with methane (CH_4) at reduced temperatures (that is, 600 to 800°C). The cells tested were 120 mm in diameter, interconnected with ferritic stainless steel. Stack operation was restricted to temperatures below 700°C; otherwise cracking of the 0.2-mm thick electrolyte occurred.

A five-cell stack was operated on 80 percent converted CH_4 . To simulate the coupling of exhaust heat with pre-reforming, as some actual SOFC systems have depicted, a reformer with integrated water evaporator was thermally connected to the stack bottom plate to reform the CH_4 . Several thermocouples were placed in fixed locations at the stack bottom plate and on the reformer walls. In addition, a flexible thermocouple was placed within the fuel supply tube and allowed temperature profiling from the reformer to the stack endplate. The reformed fuel was sampled at the reformer exit and its composition analyzed with gas chromatography. Stable performance over 2000 hours, producing 0.125 W/cm^2 , was obtained at fuel utilization between 50 percent to 70 percent and electrical efficiencies of 37 percent to 25 percent. A correlation between operating conditions and degradation was observed. The higher degradation occurred during the first 1250 hrs with high fuel utilization rates applied. At intermediate utilizations rates, the degradation rates decreased, with one cell degrading very rapidly.

A 63-cell stack was prepared and tested in a Hexis field test system. However, the stack failed under more demanding requirements of the system as a result of cell cracking. Honegger et al. (1999) concluded self-supported ceria, based SOFC cells, are not suitable for applications requiring high efficiency in operation with steam reformed methane or natural gas.

6.4 Evaluation of Material Testing, and Advanced Techniques

Wereszczak et al. (1999) performed and presented a thermal-shock strength-testing technique that has been developed using a high-resolution, high-temperature infrared camera to capture the surface temperature distribution of a specimen at the fracture. The aluminum nitride (AlN) substrates were thermally shocked to fracture for demonstrating the technique. The surface temperature distribution for each test and the AlN thermal expansion are used as input in a finite-element model to determine the thermal-shock strength for each specimen. An uncensored thermal-shock strength Weibull distribution is then determined. The test and analysis algorithm show promise as a means to characterize thermal shock strength of ceramic materials.

Lowrie and Rawlings (2000) tested two different material samples (provided by Siemens and Kerafol) of tape-cast 8 mol% yttria stabilized zirconia for microstructural stability and mechanical properties. The researchers were trying to determine how they compared related to the following two function of the electrolyte.

1. Separate the electrodes and not allowing gas leakage through the electrolyte
2. Structurally support the electrodes.

The material density, grain size, and surface finish were measured before the tests, and subsequently compared to the final test results.

Fast fracture and sub-critical crack¹ growth (sccg) tests were performed (creep² was also discovered and monitored) and as soon as the crack reached critical size, the component failed. The critical time of this crack growth was associated with critical size. Not much is found in literature about sccg of cubic YSZ, but it is known that oxides tend to be more susceptible to sccg in the presence of water and the rate is also increased at elevated temperatures.

The strength, as determined by the biaxial flexure test, was found to drop by between 23 and 30 percent on increasing the test temperature from room temperature to 950°C. They followed a DIN standard for a ring-on-ring test (a large outside ring is support for the electrolyte while a smaller inside ring is pushed through the outside ring), biaxial flexure (specifies rig and dimensions), and finite element analysis. That structure enabled the fracture stress to be calculated from the failure load, sample dimensions, and Young's modulus, E.

X-ray diffraction (XRD) was performed on the test samples at RT and up to 1100°C to determine the phases present over the temperature range. (The conclusion was the cubic phase existed over the entire temperature range of RT to 1100°C.) The X-ray texture goniometry to determine whether the tape casting produced an anisotropic microstructure showed no preferred orientation in the microstructure. The scanning electron microscope (SEM) with an energy dispersive analysis of X-ray facility (EDAX) was used to document the microstructure and measure the amount of yttria content. The SEM also detected impurities present and showed the amount of yttria varied from 7.7 mol% in Kerfol and 7 mol% in Siemens material, with no significant impurities in either material set. DIGIMAPS were plotted to show the dopant distribution. Grain sizes were measured (from SEM photographs of disc surfaces using the linear intercept technique). Densities were measured using Archimedes principle. The thermal expansion coefficient of the Siemens sample was measured using a dilatometer. Finally, the surface roughness of the samples and profile was measured using a Talysurf³.

The surface profile showed the discs were warped. The warpage was symmetrical around the center of the disc, with peak to trough values of 26 to 44 μm . The tape-casting process did not produce a microstructure with a preferred orientation, but was responsible for the surface topography and profile of the discs. The smooth surface (the side in contact with the carrier foil as the tape was cast) reflects the surface finish of the foil. The rough side was exposed to air so solvent would evaporate as the tape was dried and the binder burned out. It is believed the large porous defects close to this surface were formed during these stages; the pore clusters seen within the microstructure can also be attributed to initial sintering stages. Siemens material had fewer pores because of a slower drying rate and the rough surface. The warpage was caused by stamping that was used to produce the discs from the tape-cast sheet while it

¹ Sub-critical cracks that are initially less than the critical defect size to cause a failure, but can grow; the tests for this growth are known as sub-critical crack growth (sccg) tests.

² Creep is the increase in strain with time that a material experiences under prolonged loading. The creep rate is a function of temperature, applied stress and a parameter that depends on the material and test conditions (i.e., oxygen partial pressure in the case of oxides).

³ The Talysurf profilometer is a general purpose instrument used to measure surface profiles and surface roughness.

was still in the green stage. The tape casting process (that introduced surface defects) was found to control the initiation of fracture at RT (the strengths at RT were determined to be 290 to 350 MPa). At 950°C, the strength decreased and the processes of crack initiation and propagation had changed, no longer solely controlled by surface defects. Scgg did occur at RT and 950°C, and seemed to proceed by a grain boundary diffusion process.

A linear variable displacement transformer (LVDT)¹ was fitted to one sample and loaded under 65 MPa at 950°C to monitor the deflection as a function of time. The deflection with time recorded by the LVDT showed that after an initial region with very little deflection, a constant deflection rate of 0.2 $\mu\text{m/h}$ was attained. The total deflection was 178 μm , which agreed well with the Talysurf measurement of the disc profile at 187 μm .

The fact the material phase was cubic throughout the temperature range, plus other fairly stable conditions, indicated the electrolyte material is chemically and physically stable over the temperature range it will experience during service. Creep was also operative in this temperature range and probably was caused by a grain boundary diffusion mechanism.

The objective of the research by Taniguchi et al. (2000) was to improve the endurance of SOFC subjected to thermal cycles by reducing the stress caused by the difference in thermal expansion coefficients of the alloy separator and electrolyte. Four different test samples were constructed, labeled A through D. The first two cells, A and B, were 150- by 150-mm cells that were used to test a ceramic fiber and glass plate. A plate (made of alkaline earth borosilicate) glass was used to seal sample A. A 5-mm-wide ceramic fiber (placed on the separator side) and the same glass material used with sample A with added YSZ was used (on the electrolyte side) for sample B. The cell components were constructed of Inconel 600 separators, 200- μm -thick PSZ (3mol% Y_2O_3 + 97% ZrO_2) electrolyte. NiO anode was painted on the electrolyte, and the cathode material ($\text{La}_{0.8}\text{Sr}_{0.2}\text{MnO}_3$ 80% wt + YSZ 20% wt) was painted on the other side and sintered at 1573 K for 2 hrs. Nickel felt was used for the current collector of the anode. The tightened pressure of the cells during operation was 2 kgf/cm^2 . The gas flow rate varied by changing fuel and oxidation utilization. The A and B samples were thermal cycled from 1273 K to RT in air (at a speed of 100 K/h).

Sample A greatly degraded after one cycle. A crack found in the sample appeared to be caused by stress as a result of the difference in thermal expansion coefficients of the separator and the electrolyte. The stress was generated and increased after the glass solidified and connected the separator and the electrolyte in the cooling process. Sample B (with the ceramic fiber) displayed only small degradation after 12 cycles and no crack was found. Thus, the thermal cycle characteristics were improved by using a ceramic fiber for the sealing material. The ceramic fiber seemed to play the role of suppressing electrolyte cracking by relaxing the stress set-up during thermal cycles. However, Sample B exhibited a lower cell voltage drop and a less effective electrode area than sample A. It is believed this was caused

¹ Linear variable displacement (or differential) transformer is the basis for linear displacement transducers. An LVDT is typically an inductive device with primary and secondary coils and a ferromagnetic core. The primary core is excited when an ac voltage creates an electromagnetic field. The core links the electromagnetic field of the primary coil to the secondary coils, inducing a voltage in each.

by a gas leak that occurred through the ceramic fiber because the glass/YSZ material had proven to be a good sealing material in other research.

A follow-up method of improving the thermal cycle characteristics, while maintaining high gas seal efficiency, was investigated. The appropriate structure for the sealing material was investigated with 200 mm by 150 mm by 4 combined-cell single-layer modules. The glass was arranged around the internal manifold to suppress gas leakage. To prevent the glass from spreading during operating conditions and contacting the electrolyte, the ceramic fiber was arranged around the electrolyte.

The glass (without the ceramic fiber) spread so much that it would come in contact with the electrolyte under operating conditions. It was confirmed after thermal cycling from 1273 K to RT in air (at a speed of 100 K/h) that thermal cycle characteristics can be improved and that good cell performance can be maintained by adopting this gas seal structure. The structure that had the ceramic fiber (arranged around the electrolyte) prevented the electrolyte from contacting the glass and it did not crack.

Researchers at Rolls Royce (RR) have been involved with a number of tests for a variety of applications, and shared their mixed results¹ as applied to SOFC technology.

A test procedure may be required to measure stack performance, indicate failure, or verify models to aid in design. Depending on the requirement, the needs will be different and the type of test to meet those needs also will vary. For example, in a case where a test is set-up to detect a failed system, quantitative results are usually not needed, while they would be for a model verification test.

Some of the work performed at RR has led to the following conclusions about innovative techniques for SOFC testing. Acoustic emissions have been used for failure detection, although success is hard to predict. At Rolls-Royce vibrating-acoustic emission (AE) is used to detect broken rods in ceramic molds. The technique that involves vibrating the component and measuring the acoustic response has also been used to detect loose fittings in bearings. The problem with applying this technology to SOFC is the transducers are not capable of withstanding the high temperature. They are available for 550°C, and work is in progress to extend that to 700°C. In the absence of transducers, a wave-guide (such as a metal wire) can be used, but it may decrease the sensitivity. AE is suited to meet the need of failure detection tests.

The difficulty of optical methods is they require optical access that requires a high temperature window or fiber optics to apply the technique to the core of an operating stack. Optical methods, such as fiber optics still are temperature limited and, as such, are best suited for model validation (quantitative data) and may be useful to look at peripheral areas of the stack (such as pre-heaters or off-gas combusters).

The major advantage of optical methods is they can provide quantitative gas composition, temperature and velocity. Some of the methods are:

¹ IEA document (not publicly available). Brandon, N.P. 1995. "Acoustic and optical methods for SOFC stack testing." pp. 46-47. eds. H. Nabelek and A. McEvoy, (KFA-IEA) Research Centre Julich-International Energy Agency, Julich, Germany.

1. Laser Doppler Anemometry (LDA): gives a quantitative measure of gas velocity at a point based on the movement of fine seeding particles through crossed laser beams.
2. Particle Image Velocimetry (PIV): uses a light sheet and a double exposure image to track seeding particles, providing a vector map of the flow distribution over the region. Both PIV and LDA could be used in applications for measuring gas flows through stack components, such as verifying uniform flow distribution.
3. FTIR has been used to non-intrusively monitor the composition from engine exhaust gases using an infrared source and detector. This process is analogous to measuring the composition in the off-gas combustor of an SOFC stack.
4. Coherent Anti-Stokes Raman Spectroscopy (CARS) gives a quantitative measure of gas temperature. It has been used at RR to measure air temperatures up to 2500 K. Measurements at lower temperatures, such as 1200 K, are easier because they give a larger signal. CARS can also be used to detect some molecular species.
5. Electronic Speckle Pattern Interferometry (ESPI) provides a map of a vibrating surface that may be useful for validating mechanical models of the ceramic materials.
6. Thermal Paints: not strictly an optical method, but thermal paints do use color change to give a measure of temperature. They are used at RR to measure the temperature experienced by components in air over the range of 50 to 100°C. A single paint composition typically covers a 50 to 100°C range. Therefore, a number of paints must be used to build up a temperature map. The paints rely on post-mortem examination of the component to detect color change, but they could be useful for monitoring temperature gradients in the core of a test stack, assisting both stack design and model verifications.

In addition to these methods, thick film measurement sensors can provide useful information on the surface temperature of SOFC components during testing and operation with little disturbance. Many types of thick film temperature sensors can be used for stack control and failure detection.

Research demonstrated by Hendriksen and Bagger¹ and reported through the IEA, displayed that piezoelectric accelerometers could be used for failure detection. The accelerometers were mounted on a ceramic rod and, subsequently, the rod was pressed into a glass sealing material onto an YSZ or interconnect plate. The signal from the transducer was recorded over time and compared with the sample after it cracked (post mortem analysis). Spikes in the spectrum could be related to whether the sample was cracked or not. The method may be applicable to stacks and, with further development using a three-dimensional technique, it may be possible to determine the location of the crack. However, when

¹ IEA publication (not publicly available). P.V. Hendriksen and C. Bagger. 1995. "Concerning stack diagnostics and instrumentation: Detection of cracking by accelerometers." p. 45, eds. H. Nabielek and A. McEvoy, (KFA-IEA) Research Centre Julich-International Energy Agency, Julich, Germany.

presented at a workshop, a researcher from Sulzer Innotec Ltd. stated it had been tried on operating stacks with very noisy results. Partial oxidation (pO_2) sensors were used to measure gas composition in the inlet and outlet.

Research by Travis, Busso, and Tkach (1999) describes a methodology developed for the prediction of the thermal shock behavior of multilayer ceramic systems. An experimental procedure, based on an air flow cooling method, has been devised to typify the flow of a gas stream over the surface of a multilayered ceramic system. Such conditions are typical of SOFC operation, in particular during transient phases including start-up and shutdown. Temperatures on the surface of the tested multilayer system have been carefully monitored to calculate the corresponding stress fields. Detailed investigations of the fractured samples are presented and representative fracture patterns and crack initiation sites reported. A failure prediction methodology is presented that relies on failure diagrams constructed from a combination of experimental and analytical studies. For a given probability of failure, a diagram indicates permitted thermal shock conditions (such as temperature histories) and geometric characteristics

The test specimens were a monolayer electrolyte and multilayer (two to three layers) PEN. The PEN used for tests were 25-mm and 50-mm square, with a 200- μm thick electrolyte and 50- μm thick electrodes. The compositions were 8 mol% YSZ for the electrolyte, and Ni/8YSZ cermet for the anode and Sr-doped LaMnO_3 for the cathode.

A typical test set-up for this research is depicted in Figure 7. The specimens were heated to 950°C and then cool air was introduced through an open-ended ceramic tube inserted into the furnace. The connection of the ceramic tube to the specimen allowed the tube to move vertically at the moment when the specimen fractured. The moment of fracture was recorded as a sudden drop in temperature and the movement of the LVDT. Thermal stresses were calculated by finite element analysis for each specimen. A total of 20 monolayer electrolytes were tested and showed the fracture initiated in the center. The results were plotted using a two-parameter Weibull distribution. A fitted line and function was determined and a Weibull stress and Weibull modulus were calculated.

The multilayer PENs were tested with the same methodology, but the Weibull stress analysis was not considered appropriate and was not used. The cracks on the PENs also initiated in the center.

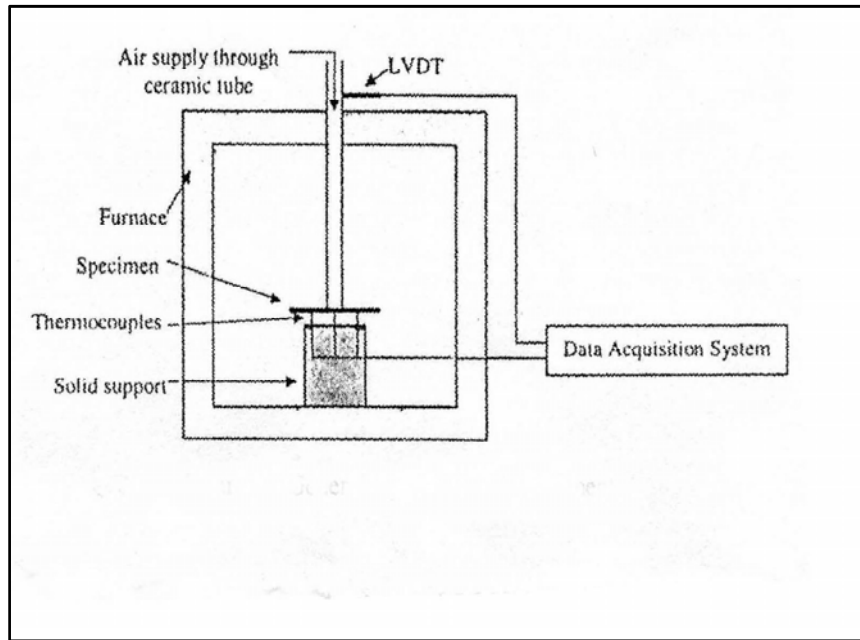


Figure 7. General Layout of the Experiment

An understanding of mechanical stresses within the fuel cell stack is required to design a fuel cell that will not exhibit poor performance or reduced lifetime. Adamson and Travis (1997) give a summary of the mechanisms responsible for generating stresses in the planar SOFC and details of the attempts made to quantify these stresses.

The SOFC is subject to large temperature changes during manufacture and operation, producing thermal mismatches between cell components. If this differential expansion in the fuel cell cannot be relaxed by allowing compliant joints between components, it must be accommodated by elastic or creep strains within the components.

The stack must be sealed at the edges to prevent the air and fuel flows from mixing. Thermal mismatches between the stack and the mountings used to support it can produce stresses within the cell components. Even the glass that is typically used to seal a PEN (in most self-supported designs) will add to the stresses. During operation, the glass is above its transition temperature, but when it cools down below the glass transition temperature, the seals become rigid (will not move) and the thermal expansion mismatch must be accommodated by the bipolar plate electrolyte and electrode.

Electrodes (of self-supported electrode-electrolyte structures) are usually manufactured by being deposited on a pre-sintered electrolyte and sintered as a unit. This method keeps the electrode from shrinking in the plane of the electrolyte by the electrolyte itself, generating tensile stresses in the electrode. The manufacturing technique of the anode involves a reduction step after sintering. This reduction step has been reported to increase the porosity of the anode, which may accommodate all of the volume change. However, if it does not, a deformation of the anode occurs.

Electrode/electrolytes are now being made that do not crack during the manufacturing process. Unfortunately, the electrode material used was chosen because of the close thermal expansion coefficient with the electrolyte material and not because it exhibits the best electrochemical behavior.

Adamson and Travis (1997) introduced a model that can predict whether cracks will propagate during manufacture. The model is based on a fracture mechanics approach and attempts to depict the effect of the residual stresses developed in the layers of the electrode-electrolyte structure. As well as the stresses that are generated during the manufacturing process, some stresses are known to generate during the operation of the SOFC, such as those caused by heat gradients and variations in partial oxygen.

The heat transfer in planar SOFC stacks is by convection, radiation, and conduction between components. The rate of cell reaction depends on the concentration of reactant gases and temperature. As the gases pass through the stack, the concentration of the gases will vary and, subsequently, the heat generated by the cell will vary and create a temperature gradient across the stack. Changes to the electrical load also influence the cell reaction, producing changes in cell temperatures. These temperature gradients cause stresses within the stack.

Models have been developed that predict the variations in temperature, gas composition, and current density in planar cells, and some of these models couple electrochemical modeling of the cell reactions with thermal modeling of the heat transfer between the gas flows and solid cell components. However, only one model (according to Adamson and Travis 1997) has been made to assess the significance of these temperature gradients. Using a finite element method, this study predicted the stresses caused by the temperature gradients across a 10-cm by 10-cm electrode-electrolyte structure.

Temperature distributions will generate stresses. An extreme temperature distribution would be expected during start-up, shutdown, and changes in the electrical load on the stack. For example, one model predicted a 400 to 500 mA/cm² increase in load would produce a maximum change in stack temperature rate of 8°C/min. Because a heating rate of 6°C per minute is often used during testing of fuel cell components, the transient stresses caused by these changes in load will not be discovered in these tests. However, in an actual emergency shutdown, or complete loss of load, could generate an even more rapid temperature change.

Some oxides show a variation in composition with oxygen partial pressure and temperature. Because the components of a SOFC are subject to different oxygen partial pressures, they will exhibit the same changes in composition. The cathode, for instance, shows changes in composition accompanied by a change in volume, and these produce an expansion mismatch with other stack components, similar to those caused by thermal mismatches. It has also been predicted that cathode material (Sr-doped LaMnO₃)

will linearly expand due to oxygen vacancy concentration; however, the author found no cases to confirm this condition.

Mechanically applied stresses are also involved in the fuel cell. The electrode-electrolyte structures are never flat after manufacture. This is partly caused by creep strains during sintering and partly the result of residual stresses. Sandwiching the PEN structure between rigid, flat bipolar plates will flatten these components, producing bending stresses and high stresses at contact points. This problem is partially relieved by placing felts between the bipolar plate and the PEN.

The theory devised by Adamson and Travis is that stress generation mechanisms acting on an individual cell may not be the same as those in a stack. In fact, it is possible that some of these stresses will mitigate others. For example, the combination of the residual stress in the electrolyte (compressive) and the point where the induced steady-state thermal stress is the greatest (tensile) will act to relieve each other. Methods to combine the many stress-causing mechanisms in a fuel cell are needed for accurate SOFC design assessment.

7.0 References

- Adamson, M. T., and R. P. Travis. 1997. "Comparison of stress generating mechanisms in a planar solid oxide fuel cell stack." 97-18, pp. 691-699. In *Solid Oxide Fuel Cells (SOFC-V): Proceedings of the Fifth International Symposium*, ed. U. Stimming. The Electrochemical Society, Pennington, New Jersey.
- Adzic, M., M. V. Heitor, and D. Santos. 1997. "Design of dedicated instrumentation for temperature distribution measurements in solid oxide fuel cells." *Journal of Applied Electrochemistry* 27(12):1355-1361.
- Appleby, A. J. 1996. "Fuel cell technology: Status and future prospects." *Energy* 21(7-8):521-653.
- Bak, J., and S. Clausen. 1999. "FTIR transmission-emission spectrometry of gases at high temperatures: Demonstration of Kirchhoff's law for a gas in an enclosure." *Journal of Quantitative Spectroscopy & Radiative Transfer* 61(5):687-694.
- Clausen, S., and J. Bak. 1998. "FTIR transmission emission spectroscopy of gases at high temperatures: Experimental set-up and analytical procedures." *Journal of Quantitative Spectroscopy & Radiative Transfer* 61(2):131-141.
- Condensed Matter Department of Universiteit Utrecht. EIS: Electrical Impedance Spectroscopy. 2001. <http://www.chem.uu.nl/gm/www/eis.html>
- Edwards, D. D., J-H. Hwang, S. J. Ford, and T. O. Mason. 1997. "Experimental limitations in impedance spectroscopy: Part V Apparatus contributions and corrections." *Solid State Ionics*, pp. 85-93.
- Elangovan, S., J. Hartvigsen, S. C. Kung, R. W. Goettler, and E. A. Barringer. 2001. "Planar solid oxide fuel cell development at SOFCo (SOFC VII)." vol. 2001-16, pp. 94-99. In *Solid Oxide Fuel Cell VII*, eds. H. Yokokawa and S. C. Singhal. The Electrochemical Society Inc., Pennington, New Jersey.
- Ellis, M. W. 2000. *Fuel Cell Cogeneration Technology Assessment Guide*. ASHRAE Research Project 1058-RP and cooperation with technical committee TC 9.5 Cogeneration Systems, Atlanta, Georgia.
- Gardner, F. J., M. J. Day, N. P. Brandon, M. N. Pashley, and M. Cassidy. 1999. "SOFC technology development at Rolls-Royce." *Journal of Power Sources* 86(1-2):122-129.
- Godfrey, B., K. Foger, R. Gillespie, R. Bolden, and S.P.S. Badwal. 2000. "Planar solid oxide fuel cells: the Australian experience and outlook." *Journal of Power Sources* 86(1-2):68-73.
- Guillodo, M., P. Vernoux, and J. Fouletier. 2000. "Electrochemical properties of Ni-YSZ cermet in solid oxide fuel cells, effect of current collecting." *Solid State Ionics*, pp. 99-107.

- Hartvigsen, J., C. Milliken, S. Elangovan, and A. Khandkar. 1996. "Challenges to obtaining high efficiency in solid oxide fuel cells." pp. 279-291. In *Role of Ceramics in Advanced Electrochemical Systems*, ed. The American Ceramic Society, Westerville, Ohio.
- Hirschenhofer, J. H., D. B. Stauffer., R. R. Engleman., and M. G. Klett. 1998. *Fuel Cell Handbook Fourth Edition*. U.S. Department of Energy, Office of Fossil Energy, Federal Energy Technology Center, Morgantown, West Virginia.
- Honegger, K., R. Kruschwitz, M. Keller, and G. M. Christie. 1999. "Performance of SOFC stacks operated with CH₄ at reduced temperatures (600-800°C)." 99-19, pp. 1019-1026. In *Solid Oxide Fuel Cells (SOFC-VI): Proceedings of the Sixth International Symposium*, eds. S.C. Singhal and M. Dokiya. The Electrochemical Society, Pennington, New Jersey.
- Khandkar, A.C., S. Elangovan, and J.J. Hartvigsen. 1996 "Progress in planar SOFC science and technology" pp. 263-276. In *Role of Ceramics in Advanced Electrochemical Systems*, ed. The American Ceramic Society, Westerville, Ohio.
- Larminie, J. and A. Dicks. 2000. *Fuel Cell Systems Explained*. John Wiley & Sons, Ltd., New York.
- Lequeux, G. 2001. "Status of the European Programme (SOFC VII)." vol. 2001-16, pp. 14-27. In *Solid Oxide Fuel Cell VII*, eds. H. Yokokawa and S. C. Singhal. The Electrochemical Society Inc., Pennington, New Jersey.
- Lindeburg, M. R. 1990. *Mechanical Engineering Reference Manual Eighth Edition*. Professional Publications, Inc., Belmont, California.
- Lowrie, F. L., and R. D. Rawlings. 2000. "Room and high temperature failure mechanisms in solid oxide fuel cell electrolytes." *Journal of the European Ceramic Society* 20(6):751-760.
- Mogensen, M., P. H. Larsen, P. V. Hendriksen, B. Kindl, B. Carsten, and S. Linderorth. 1999. "Solid oxide fuel cell testing: results and interpretation." 99-19, pp. 904-915. In *Solid Oxide Fuel Cells (SOFC-VI): Proceedings of the Sixth International Symposium*. eds. S.C. Singhal and M. Dokiya. The Electrochemical Society, Pennington, New Jersey.
- Primdahl, S., P. V. Hendriksen, P. H. Larsen, B. Kindl, M Mogensen, and (SOFC VII). 2001. "Evaluation of SOFC test data." vol. 2001-16, pp. 932-941. In *Solid Oxide Fuel Cell VII*, , eds. H. Yokokawa and S. C. Singhal. The Electrochemical Society Inc., Pennington, New Jersey.
- Pyke, S. H., and G. Lequeux. 2001. "Distributed power generation plant based on planar SOFC, proof of concept." http://fuelcellnetwork.bham.ac.uk/papers/Distrib_gen_SOFC.htm
- Ringuede, A., J. Fouletier, and L. Dessemond. 2000. "Impedance spectroscopy study of SOFC cathodes." pp. 283-294, In *Fourth European Solid Oxide Fuel Cell Forum*, ed. A.J. McEvoy. European Fuel Cell Forum, Oberrohrdorf, Switzerland.

Sakaki, Y., A. Nakanishi, M. Hattori, H. Miyamoto., H. Aiki, and K. Takenobu. 2001. "Development of MOLB type SOFC (SOFC VII)." vol. 2001-16, pp. 72-77. In *Solid Oxide Fuel Cell VII*, eds. H. Yokokawa and S. C. Singhal. The Electrochemical Society Inc., Pennington, New Jersey.

Singhal, S. C. 2001. "Low cost modular SOFC system development at Pacific Northwest National Laboratory (SOFC VII)." vol. 2001-16, pp. 166-172. In *Solid Oxide Fuel Cell VII*, eds. H. Yokokawa and S. C. Singhal. The Electrochemical Society Inc., Pennington, New Jersey.

Taniguchi S., M. Kadowaki, T. Yasuo, Y. Akiyama, Y. Miyake, and K. Nishio. 2000. "Improvement of thermal cycle characteristics of a planar-type solid oxide fuel cell by using ceramic fiber as sealing material." *Journal of Power Sources* 90:163-169.

Travis, R.P., E.P. Busso, and Y.V. Tkach. 1999. "Thermal shock resistance of multilayered ceramic components." 99-19, pp. 1037-1045. In *Solid Oxide Fuel Cells (SOFC-VI): Proceedings of the Sixth International Symposium* eds. S. C. Singhal and M. Dokiya. The Electrochemical Society, Pennington, New Jersey.

Virkar, A.V., J. Chen, C.W. Tanner, and J-W. Kim. 1999. "The role of electrode microstructure on activation and concentration polarizations in solid oxide fuel cells." *Solid State Ionics* 131:189-198.

Wereszczak, A.A., R.A. Scheidt, M.K. Ferber, and K. Breder. 1999. "Probabilistic thermal-shock strength testing using infrared imaging." *Journal of the American Ceramic Society* 82(12):3605-3608.

Williams, M.C. 1997. "U.S. solid oxide fuel cell power plant development and commercialization (SOFC V)." vol. 97-18, pp. 3-11. The Electrochemical Society Inc., Pennington, New Jersey.

Yasuda, I. 2001. "Solid Oxide Fuel Cells (SOFC)." http://www.tokyo-gas.co.jp/techno/stp/e_txt/193.htm

Distribution

**No. of
Copies**

15 Pacific Northwest National Laboratory

L. Bond	K5-26
L. Chick	K2-44
J. Hartman	K5-25
A. Hess	K7-30
D. Hurley	K5-22
D. Jarrell	K5-20
P. Singh	K2-50
S. Singhal	K2-18
Information Release (7)	K1-06